THE UNIVERSITY OF MICHIGAN

INDUSTRY PROGRAM OF THE COLLEGE OF ENGINEERING

ON DETERMINING THE HARDNESS OF GRINDING WHEELS-I

L. V. Colwell
R. O. Lane
K. N. Soderlund

April, 1961

IP-508

en bn

UNRC681

ACKNOWLEDGEMENTS

The authors are grateful to the Macklin Company of Jackson, Michigan for furnishing the cutters and cutter spindle used during this investigation and for supplying many of the grinding wheels needed for the study. We also wish to thank Mr. Robert Franklin, president of the Macklin Company for his encouragement and continued interest in this activity.

Special credit is due three Mechanical Engineering students who worked many extra hours because of their enthusiam and eagerness to make a contribution to engineering. These men are C. Arthur Carlson, Raymond A. Jacobson and Dean R. Metzger. All were students in the Production Engineering Laboratory at the University of Michigan.

TABLE OF CONTENTS

	Page
ACKNOWLEDGEMENTS	ii
LIST OF TABLES	iv
LIST OF FIGURES	v
ABSTRACT	vii
ON DETERMINING THE HARDNESS OF GRINDING WHEELS - I.	1
Functional Hardness of Grinding Wheels	1
System Rigidity as a Factor	2
Elastic Modulus of the Wheel as a Factor	3
Elastic Support of Individual Grains as a Factor	3
Wheel Wear as a Factor	4
Effective Hardness Defined	4
Laboratory Investigation	10
Test Results	12
Measured Hardness vs. Bending Strength	17
Analysis and Interpretation	29
The Crushing Component	29
The Elastic Component - P_e	36
The "Packing" Component - P_p	38
The Total Force - F	39
Testing the Equation	39
Application	45
Quality Control	45
An Industrial Standard	47
The Effect of Speed	52
Summary	55
APPENDIX	57
I. Geometry of the Contact Zone	57
II. Area of the Contact Zone	59
III. Velocity of Approach	62
IV. Elastic Contact Conditions	64
BIBLIOGRAPHY	67

LIST OF TABLES

Table		Page
I	Strength Data on Wheels Studied.....	18
II	Calculated Crushing Pressures - (ρ) at Four Different Test Conditions.....	19
III	Grain Constants and Concentration Coefficients.....	33
IV	Summary of Crushing Force Equations.....	35
V	Standard Proportions of Abrasive, Bond and Porosity...	41
VI	Forces and Ratios for Two-Pass Procedure.....	51
A	Values of X_1 and Y_1 at Test Conditions.....	61
B	Approach Velocities During Crushing.....	63
C	Elastic Properties of Wheels.....	65
D	A Comparison of Contact Pressures and Areas for (Vitrified and Resinoid Grinding Wheels).....	65

LIST OF FIGURES

Figure		Page
1	The influence of elastic deformation of bond posts on effective grain spacing.....	6
2	Effective grain spacing as a function of depth of cut for several different grain sizes in vitrified aluminum oxide wheels while surface grinding steel with cup shaped wheels.....	9
3	A schematic of the laboratory test set-up.....	11
4	Test results of 12 x 1 x 5 vitrified, aluminum oxide grinding wheels differing only in grain size...	13
5	Results for wheels differing only in structure.....	14
6	Results for wheels differing only in grade-60 Grit, 5 structure.....	15
7	Results for wheels differing only in grade-46 Grit, 8 structure.....	16
8-15	Calculated pressure in the crushing zone from Table II versus bending strengths from Table I.....	21-28
16	Front view of probable conditions in the contact zone between the crushing wheel and the grinding wheel.....	30
17	Shows the increase in the number of abrasive grains per unit area in the cutting zone as the depth of cut in actual grinding is increased.....	32
18-20	Crushing force for variable depth and feed at four different values of constant feed and four different values of constant depth for the same abrasive wheel.....	42-44
21	A reproduction of actual test record for the circumference of a defective grinding wheel.....	46
22	Plot of crushing forces on successive passes in a procedure wherein the cross-slide was adjusted inward on every other pass.....	48
23	Relationship of force on second pass to that for the first pass in the two-pass procedure.....	53

LIST OF FIGURES (CONT'D)

Figure		Page
24	Effect of speed on test results.....	54
A	Illustrates the essential geometry in the crushing zone.....	58
B	Shows the geometric relationship between the radial crushing depth-d and the height-Y_1 of the contact zone.....	60

ABSTRACT

A new method for evaluating the hardness of grinding wheels has been developed. It involves crushing small amounts of abrasive from the surface of a grinding wheel while in rolling contact with a hard steel wheel. Measured reaction forces provide a sensitive indication of significant variations in the hardness as well as other important properties of bonded abrasives.

A laboratory analysis of the method demonstrates that the hardness values incorporate the same elastic constants which have been shown to be important in actual grinding. The analysis shows also that it is feasible to establish a universally applicable industrial standard for grinding wheel hardness.

The method is valuable also as a research tool and may be expected to aid in producing more uniform abrasive products and to yield information which will help improve practices in the manufacturing plant.

ON DETERMINING THE HARDNESS OF GRINDING WHEELS - I

The problem of measuring the hardness of grinding wheels has been the object of numerous investigations for more than 40 years. Several techniques have arisen from these studies but the fact that new investigations have repeatedly been started is mute testimony to the effect that the problem has not been solved sufficiently to meet the need.

Considered generally, hardness as a property of grinding wheels has substantially the same significance as hardness of metals as measured by the well known Brinell and Rockwell procedures. The functional hardness of metals involves strength and load-carring ability, ability to absorb shock and ability to resist wear. To a very limited extent this is true also for grinding wheels and other bonded abrasives. But the similarity ends here for two very important reasons. One reason concerns significant differences in the definition of functional hardness as between metals on the one hand and bonded abrasives on the other. The other reason although not entirely independent of the first involves the essentially coarse-grained, heterogeneous nature of bonded abrasives as compared to metals.

Functional Hardness of Grinding Wheels

In order to define functional hardness competently one must begin in the production shop where grinding wheels are used. Here one observes that a grinding wheel may be moved from one grinding machine to another and be judged to act harder despite the fact that the wheel as a

structure and its real hardness remain unchanged. The increase in apparent or functional hardness is nonetheless real since it was the result of a decrease in overall system rigidity or stiffness of which the hardness of the grinding wheel is only one part.

System Rigidity as a Factor

The system, consisting of the grinding wheel, the machine, work holding devices and the work piece constitute a group of elastic springs loaded in series. The grinding wheel can be thought of as a simple compression spring in series with several other compression springs. Under load all will deflect; each by an amount inversely proportional to its stiffness. If any one of the springs is replaced by a softer or more flexible spring, all others in the series act harder or stiffer relative to the overall stiffness of the system.

Thus it is only natural that the functional hardness of a grinding wheel will change as other elements of the system change. A stiffer machine makes a particular wheel act softer; a machine of lower stiffness makes the same wheel appear to be harder. Similarly, relatively rigid work pieces and work holding fixtures make a wheel act soft whereas the same wheel behaves as though it were harder when the elastic stiffness of either the workpiece or the fixture is reduced.

Up to this point in the qualitative analysis of functional hardness of grinding wheels it appears that elastic properties play a dominant role in contrast to penetration hardness of metals where plastic flow is a major factor.

Elastic Modulus of the Wheel as a Factor

It is also well known in production shops that other factors being equal, a resinoid bonded grinding wheel will act much harder than a wheel with a vitrified bond. This appears superficially to be something of a paradox since a resin bonded wheel is indeed much softer structurally than a vitrified wheel. The elastic modulus of a vitrified wheel may be from three to six times as large as that of a resinoid wheel.

However, this property operates in precisely the same manner as the other elastic elements of the system. After all, it is the individual abrasive grain which is the active cutting tool and so if a softer, springier grinding machine will make it act harder than so also will a lower elastic modulus of the grinding wheel itself.

Elastic Support of Individual Grains as a Factor

On the basis of present knowledge, one can only speculate as to the influence of this factor except to say that a softer, springier support certainly will make the grain act harder. It must be true also that the elastic properties of individual grain supports vary directly with the elastic modulus of the wheel but behavior locally in the immediate vicinity of each grain may depend strongly upon grain size, porosity, ratio of volume of bond to volume of abrasive as well as some other factors as yet unidentified. Consequently, the elastic properties of individual grain supports may be substantially unique compared to those of the wheel as a whole in which case they must also be considered as another set of independent variables in the composite property called effective hardness.

Wheel Wear as a Factor

We come next to the simplest of the properties involved in overall effective hardness. It is also the property which has caused the word hardness to be used rather paradoxically in describing influences that amount fundamentally to increased softness rather than increased hardness.

As abrasive grains wear, they become dull. The duller they become the higher forces build up before they will cut. Also greater frictional heating will result. Eventually, the forces on individual grains may build up until the grain itself fractures or the whole grain is broken out of the structure thus presenting new and sharp cutting edges.

Fundamentally then, other factors being equal, a truly harder grinding wheel is one which hangs on to a dull abrasive grain to a higher degree of dullness thus creating greater forces which in turn can make it more difficult to control size. The greater frictional heat also aggravates quality control of the grinding process through both size control and sensitivity to grinding cracks and other manifestations of thermal damage.

It should be noted in summary that this property is not singularly unique but that it involves the strength and friability of the abrasive material itself as well as the combined strengths of the bond posts. Either one factor or the other may dominate in specific instances. Doubtlessly both factors operate concurrently in others.

Effective Hardness Defined

In summary, a qualitative definition of functional or effective hardness of bonded abrasives and grinding wheels must include at least

the following variable factors:

No. 1) Terminal dullness of individual abrasive grains

No. 2) Elastic properties of individual grain supports

No. 3) Elastic properties of the bonded abrasive as a body or structure

No. 4) Combined elastic properties of the entire system.

The first of these is essentially a hardness or strength type of factor. The undesirable consequences of greater dullness or the corresponding hardness is augmented and aggravated by the presence of the three elastic factors.

The dullness factor is a property of individual grains. However, the total consequences of dulling is determined by how many dull grains are in contact with the workpiece at the same time. This is influenced by factors "2" and "3" above as well as by the geometry and size of the machining operation being performed by bonded abrasives. The other elastic components that go to make up system rigidity influence "spark-out" characteristics in grinding, dwell behavior and other phenomena which affect size control, surface finish and tendency toward chatter.

Peklenik[1]* emphasized these same elastic factors in his excellent analysis of the criteria and parameters which must be considered in evaluating grinding behavior. This is illustrated schematically in Figure 1.

Here in exaggerated form one sees a grinding wheel in idealized form wherein each abrasive grain is supported by its own spring which will

* Numbers in parentheses correspond to references cited in the bibliography.

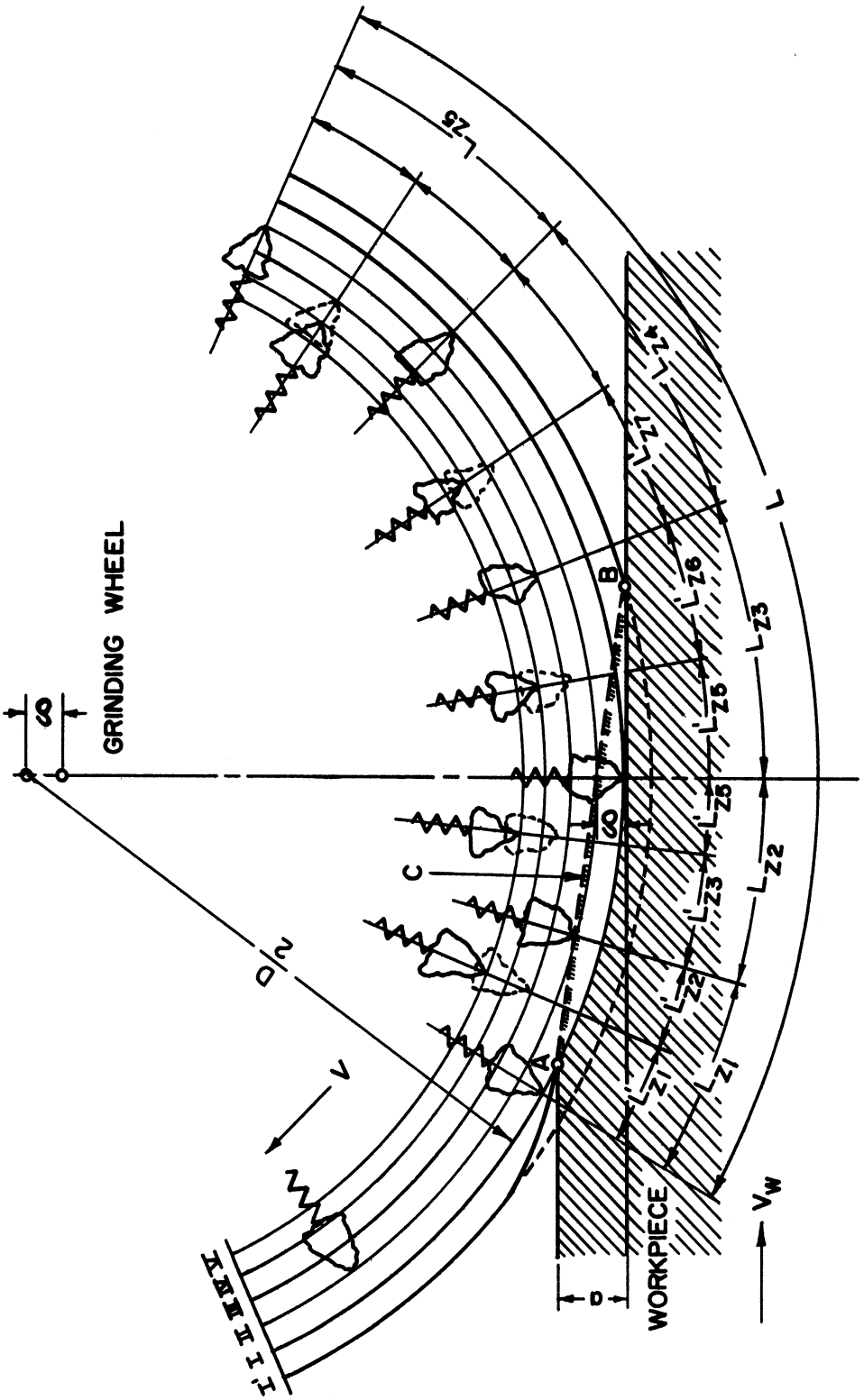

Figure 1. The influence of elastic deformation of bond posts on effective grain spacing. Each combination of bond posts is represented by a simple spring so far as radial deflection is concerned. (From the dissertation by J. Peklenik, Reference 1)

permit it to deflect radially toward the center of the wheel. The arrangements simulate flat surface grinding with the wheel rotating clockwise and the workpiece in motion from left to right.

If the system were infinitely rigid, the wheel would cut a path as shown by the dashed line connecting point B with the original work surface. However, the system rigidity is finite so that the center of rotation deflects an amount-δ relative to the workpiece. This is the fourth of the four factors cited previously as an element of effective hardness.

The contact surface through point A would be substantially cylindrical if the modulus of elasticity of the wheel, (factor No. 3) were infinite. However, this surface tends to flatten-out and lengthen as designated by the dashed line - ACB. This increases the area of contact which in turn, increases the number of dull grains in contact with the work. Obviously, the lower modulus of a resinoid wheel would cause the area to be larger than that for a vitrified wheel at the same depth of cut. It should be noted also that higher modulus of elasticity of the work material would have the same effect. Consequently the increase in contact area and the corresponding increase in effective hardness must vary directly as some function of modulus of elasticity of the work divided by the modulus of elasticity of the wheel.

If one were to select a particular plane of a grinding wheel as in Figure 1 and count the number of abrasive grains at precisely the same radius within plus or minus a millionth of an inch for example he would find very few grains at this radius around the entire circumference. In other words the distance or spacing-L between grains following each other

in identical paths is relatively large at light loads. As loads are increased by increasing depth of cut, the individual grains deflect by amounts proportional to Factor No. 2 with the result that more grains are concentrated at the same radius.

One result of this concentration is a reduction in the average or effective grain pitch or spacing. This is predicted by Figure 1. Figure 2 shows the results of actual measurements of this property as reported by Peklenik[1] for flat surface grinding of steel with vitrified cup wheels of aluminum oxide abrasive. It is clear from these results that local deformation characteristics, Factor No. 2 will have a separate and unique effect upon the number of dull grains in contact with the work surface. In addition to the effect of grain size as shown in Figure 2 one can well expect additional effects from variations in ratios of bond to abrasive and porosity. These might well affect the deformation characteristics of individual grains as well as the modulus of elasticity of the bonded structure as a whole. However, this area requires much more work of the type done by Peklenik before these questions can be answered in a quantitative manner.

It appears then that any procedure intended to predict the functional or effective hardness of grinding wheel as it will behave in actual grinding must be sensitive to the elastic properties as well as to the force required to fracture or break out dull abrasive grains. A laboratory study of this problem has been made and analysis of the results indicates that it is possible to incorporate the elastic factors in a test for effective hardness.

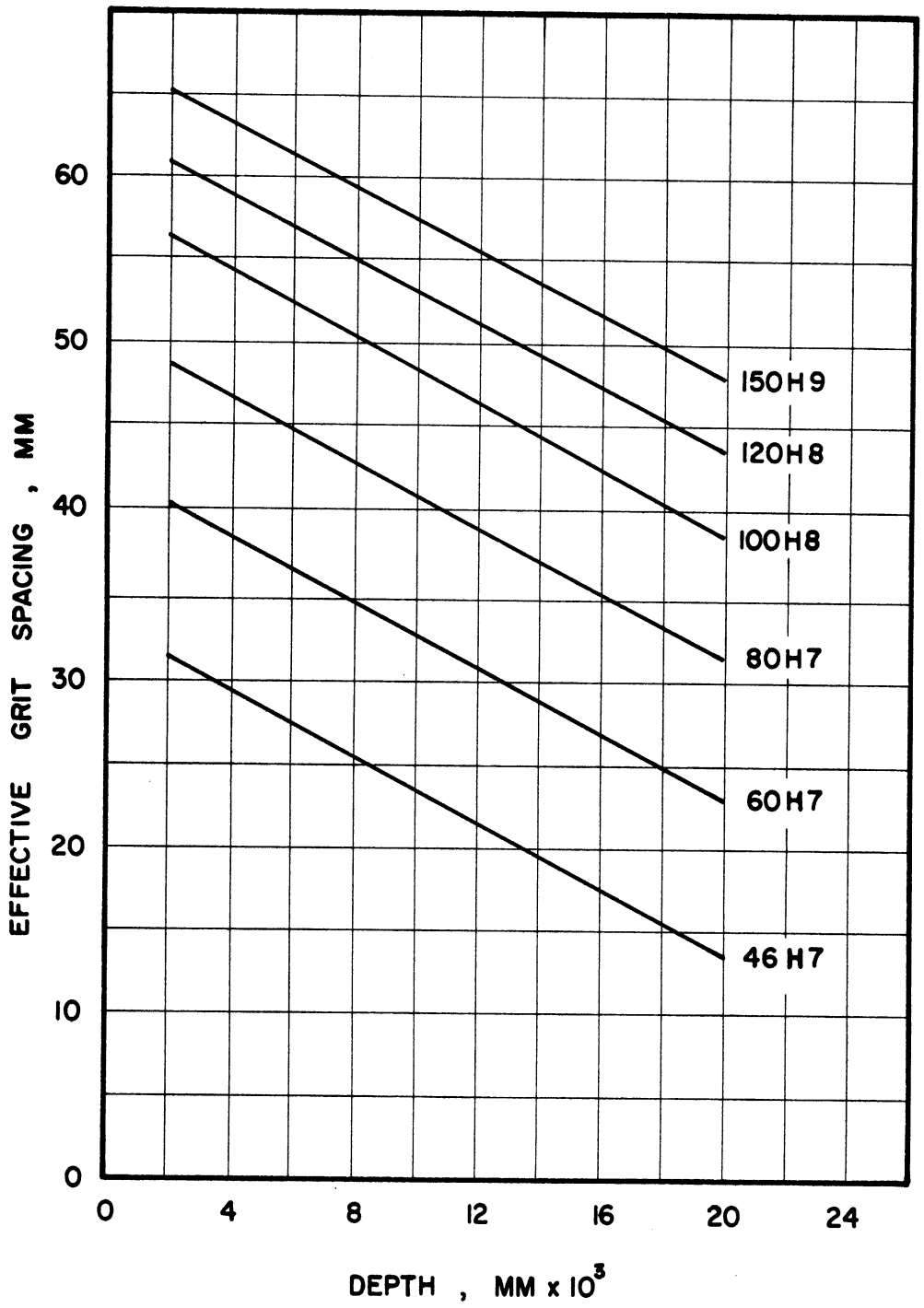

Figure 2. Effective grain spacing as a function of depth of cut for several different grain sizes in vitrified aluminum oxide wheels while surface grinding steel with cup shaped wheels. Wheel speed = 4150 sfpm. Work speed = 118 ipm. (From the dissertation by J. Peklenik, Reference 1)

Laboratory Investigation

A laboratory study was carried out on this problem using the set-up shown schematically in Figure 3. Wheels 12 x 1 x 5 were mounted on an adapter fastened to the driving plate of a 12-inch swing engine lathe. A cutter or crushing wheel consisting of a 90 degree included angle, conical cup with 0.100 inch thick wall is mounted on a free-running spindle. The centerline of the spindle intersects the centerline of the lathe spindle at an angle of 45 degree. The cutter spindle is mounted on a two-component lathe dynamometer which in turn is fastened to the cross-slide by means of a suitable adapter. The dynamometer measures forces both vertically and horizontally.

Crushing or cutting of the abrasive wheel is accomplished by setting the cross-slide for the desired depth and then feeding the cutter across the face of the abrasive wheel in either direction. The surface velocities of the two wheels are the same and true rolling takes place. This process of cutting or crushing is used by some grinding wheel manufacturers to true up wheels after they are fired or cured.

It was reasoned that the elastic forces which must be built up before crushing can occur would at least reflect the properties outlined in the previous section. A series of exploratory tests were carried out with a group of vitrified aluminum oxide wheels representing variations in grain size, structure and grade. Feed rate was varied at a constant depth of 0.006 inch and depth was varied at a constant feed rate of 0.052 ipr. All tests were carried out at a constant spindle speed of 700 rpm. Each test was repeated until the measured forces leveled-off at an appropriate maximum value; this usually occurred no later than the third run but was confirmed by a fourth run.

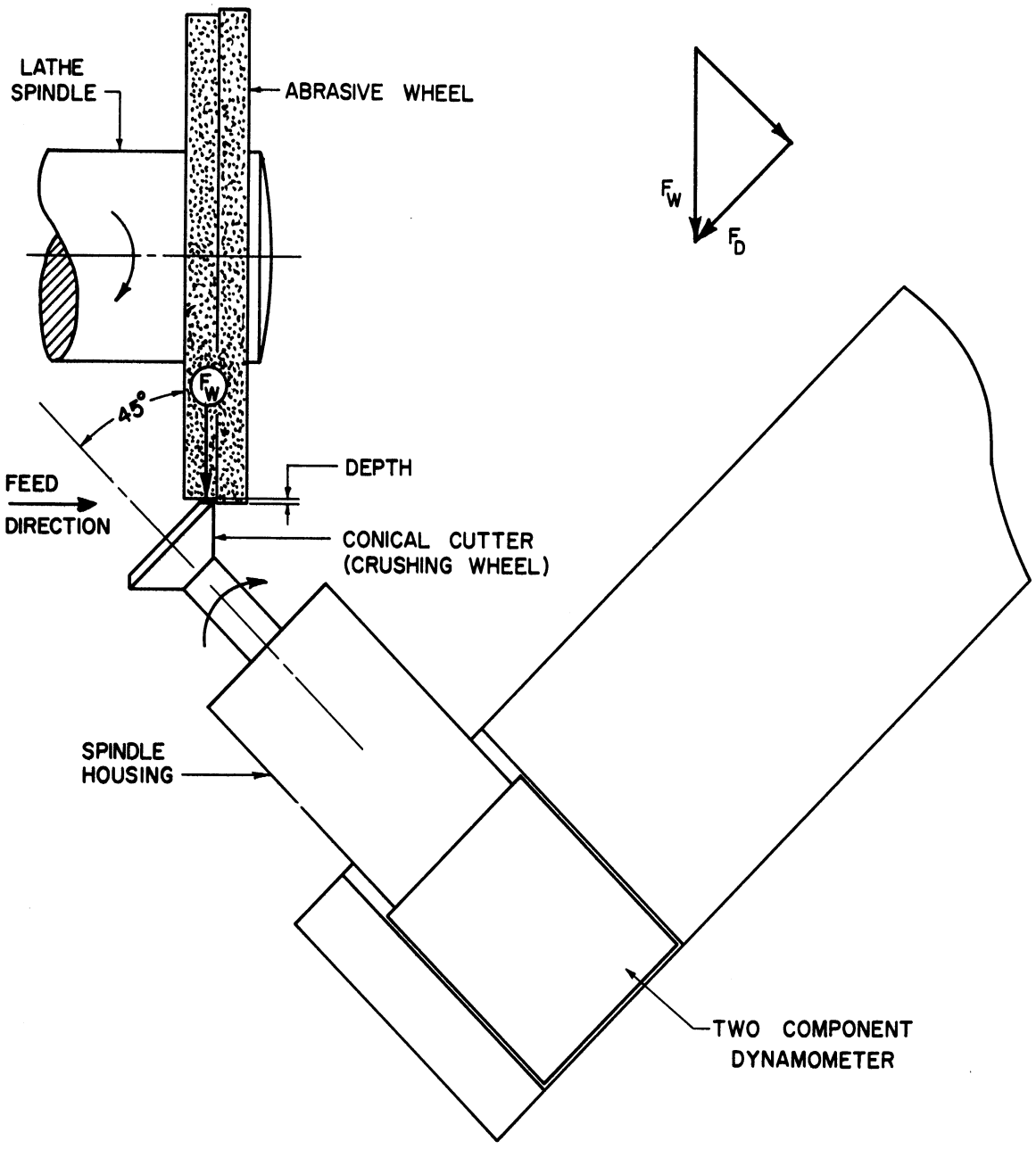

Figure 3. A schematic of the laboratory test set-up. The dynamometer is mounted on an extension plate substituted for the compound of a modified 12 inch swing engine lathe. Depth settings were made with the cross-slide and feeding was accomplished with the carriage. Vertical and horizontal force components were indicated on the chart of a Model 60 Sanborn carrier-amplifier-recorder. Crushing wheel is SAE6150 steel hardened to 54-56 Rockwell C-scale.

Test Results

The results of this series are shown plotted on logarithmic coordinates in Figures 4-7 inclusive. Figure 4 gives the results for wheels differing only in grain size. The measured horizontal forces are plotted against corresponding feeds and depths. In all cases the vertical component of force on the dynamometer was negligible and barely measurable except for the very short period during which the cutter was accelerated to full speed.

The first thing to be noted about all the data in Figures 4-7 is the orderly change in crushing force as both the feed and depth are changed. In reference to Figure 4, it is interesting to note two further points. The first is that the slopes of the variable feed lines are greater than the slopes of the variable depth lines. The second is that the slopes decrease with decrease in grain size. Possible reasons for the different slopes are discussed later.

Figure 5 shows the results for a series of wheels differing only in structure. There was a substantial drop in force in going from the No. 5 structure to a No. 8 structure. However a further change in the same direction to a No. 12 structure resulted in a higher hardness. Attention is called to the equation for the wheel with the No. 8 structure. Later on it will be shown that this equation can be predicted almost entirely from known behavior in actual grinding.

Figure 6 shows the results for a group of wheels differing only in grade or hardness. The O-Grade wheel was almost too hard for the laboratory apparatus since it had a strong tendency to chatter at

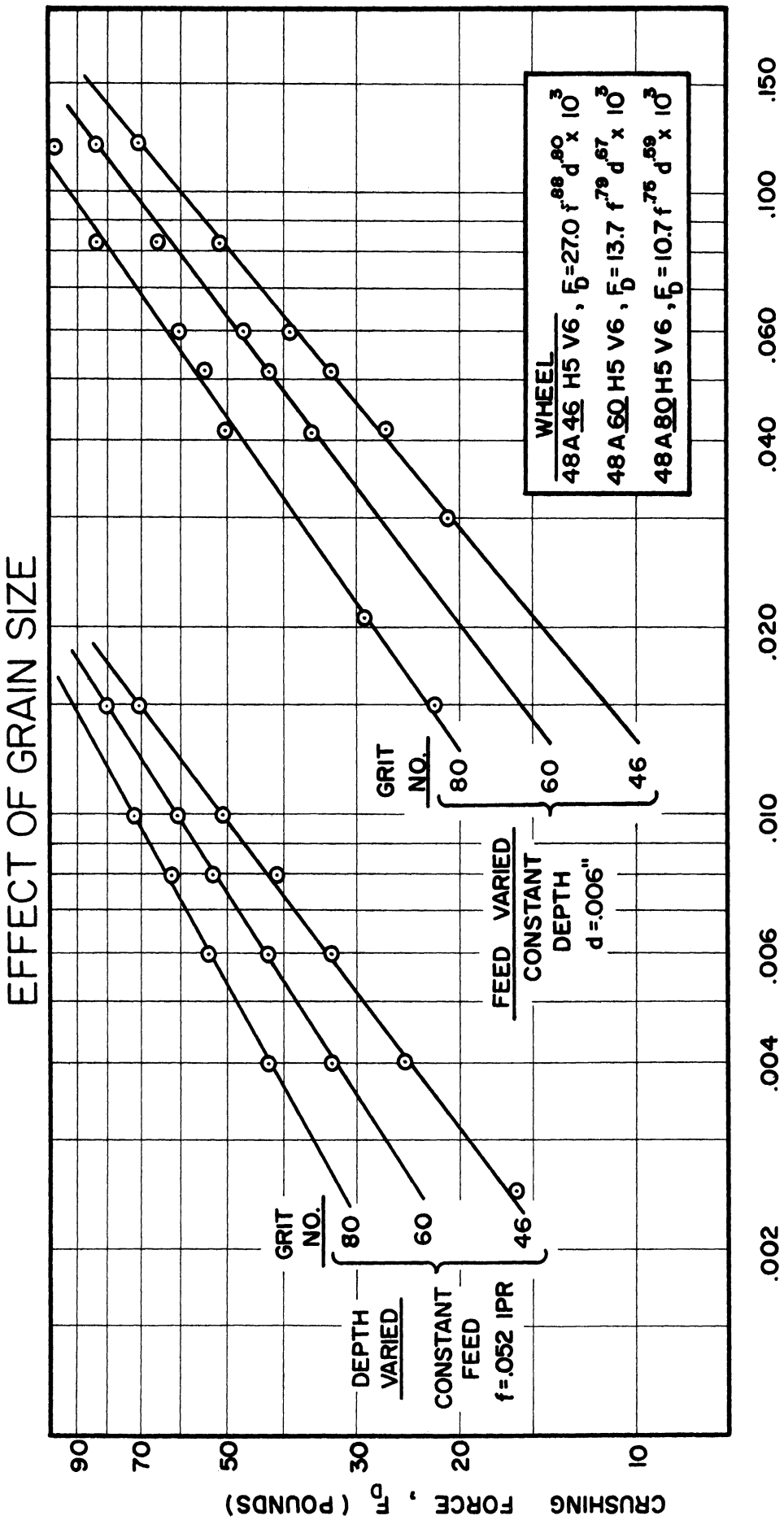

Figure 4. Test results of 12 x 1 x 5 vitrified, aluminum oxide grinding wheels. All were made to the same specifications except for grain size. Test points shown are the equilibrium averages of at least three consecutive tests. Vertical force component was negligible. Speed constant at 700 rpm.

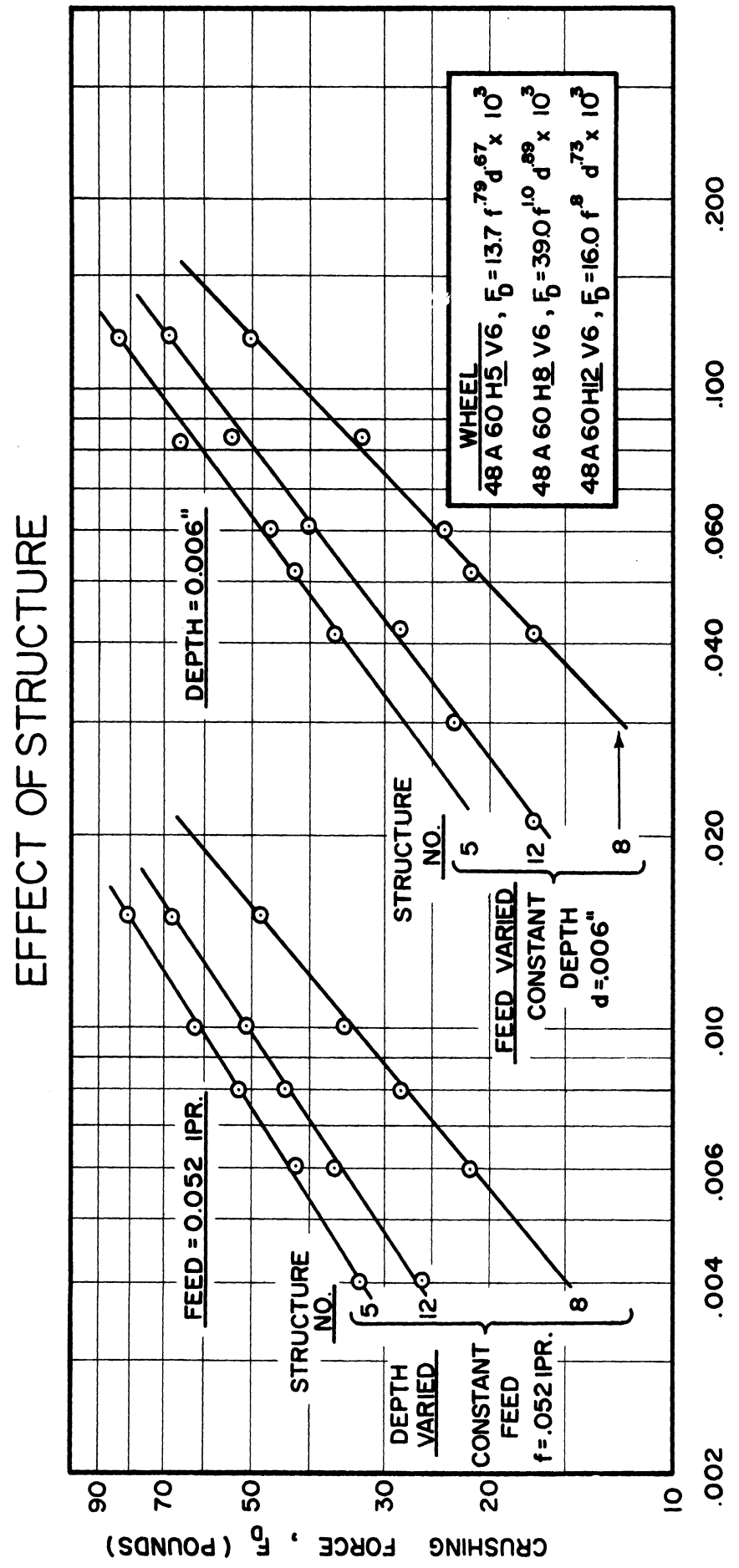

Figure 5. Results for wheels differing only in structure. Larger structure numbers indicate larger percentage of bond and lower percentage of abrasive. Porosity remains constant with grade. (See Table V) Test conditions same as in Figure 4.

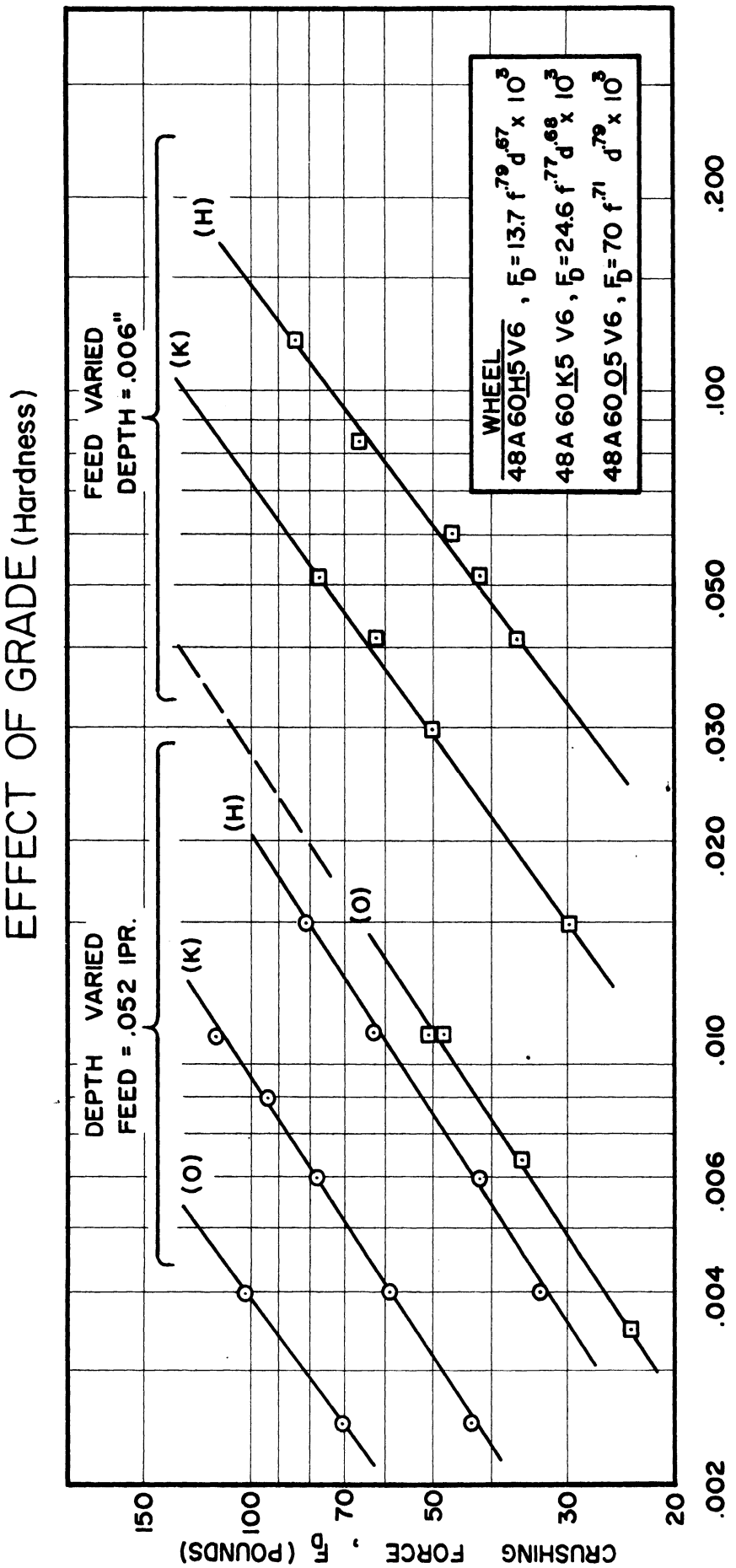

Figure 6. Test conditions same as in Figure 4. Wheels differed only in grade or hardness except that the O-wheel was 1¼ inches in diameter and had V7 bond which contains a little iron and is somewhat weaker than V6 bond. Dynamometer had tendency toward chatter at heavy cuts on the O-wheel.

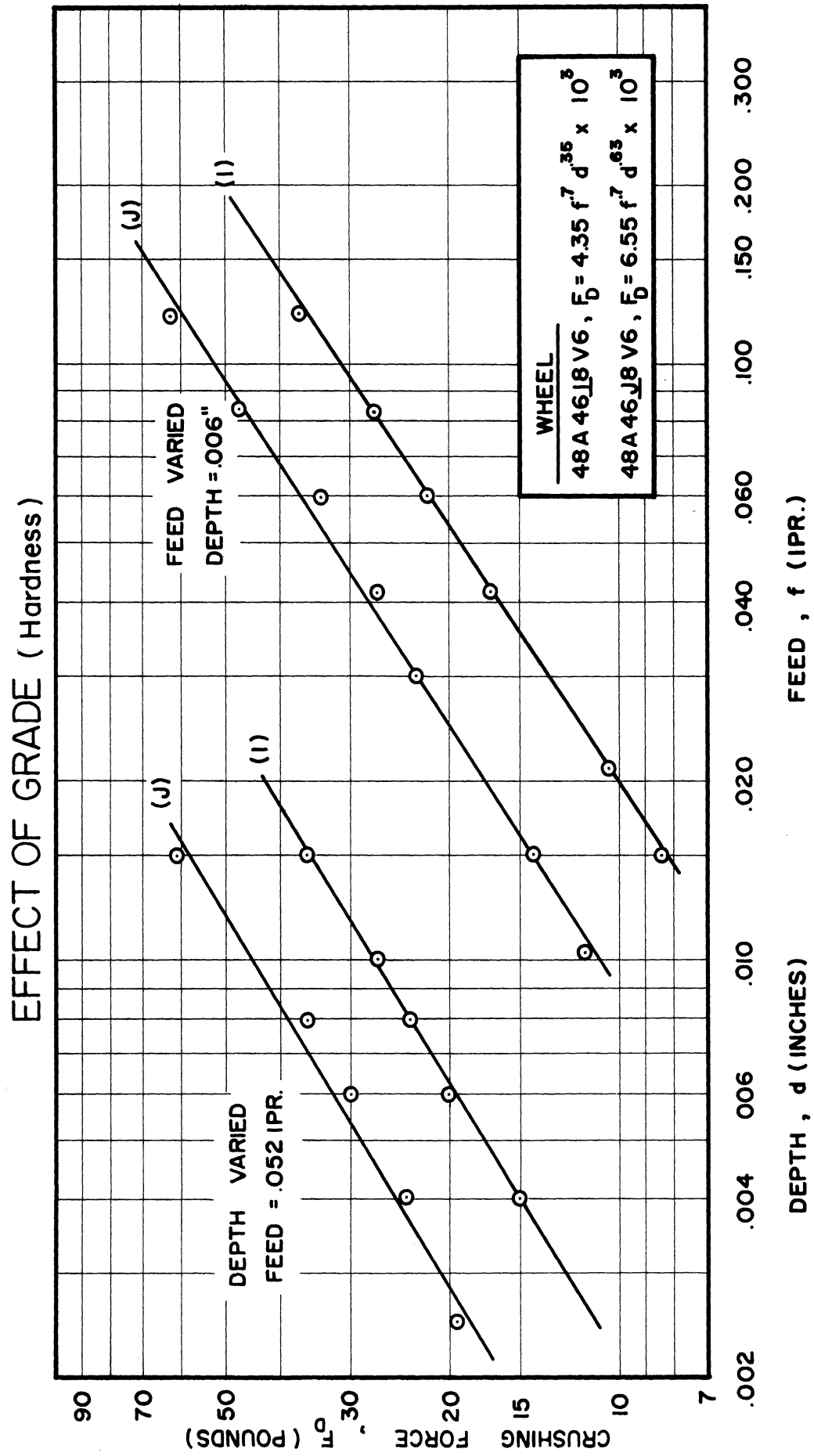

Figure 7. Similar to wheels in Figure 6 except that structure is softer and grain size is larger. Test conditions same as in Figure 4.

forces above 120-130 pounds. It will be shown later that these lines should remain substantially parallel when only the grade is varied.

Figure 7, shows the results for two adjacent grades in a different grain size and structure than the wheels represented in Figure 6. Once more the lines are nearly parallel within each set.

Measured Hardness vs. Bending Strength

As a part of early exploration, a search was made for possible correlation of some function of the measured forces and the bending strength of the wheels. The bending strengths of all of the grinding wheels represented in Figures 4-7 were determined from the averages of eight tests on each wheel. The results are summarized in Table I.

In addition, average crushing pressures were calculated on the assumption that the total force measured in the tests was concentrated in the crushing zone. The results of these calculations are summarized in Table II. The force indicated from dynamometer calibration, F_D, was first multiplied by $\sqrt{2}$ to get the actual force - F_W. Then the actual force was divided by the area of the crushing zone as represented by Equation (B-5) in the Appendix.

Apparent crushing pressures were calculated for four different sets of test conditions designated as A, B, C, and D in Table II. A comparison of the pressures in columns A and C shows an apparent drop in pressure as the feed is increased. This indicates that there is an elastic component of the force and it does not increase linearly with the feed. Furthermore at least part of the elastic component must arise outside the crushing zone.

TABLE I

STRENGTH DATA ON WHEELS STUDIED

Wheel	Breaking Load - p (lbs)	b (in.)	t (in.)	bt^2	2σ - (psi)
48A60H5V6	1022	1.003	1.104	1.225	8,350
- 60H8 -	1087	.968	1.254	1.521	5,950
- 60H12-	877	1.010	1.174	1.392	5,650
- 60K5 -	1410	1.015	1.052	1.128	11,250
- 46H5 -	896	1.016	1.039	1.090	7,400
- 80H5 -	1393	1.004	1.136	1.295	9,700
- 46I8 -	760	1.048	1.040	1.136	6,000
- 46J8 -	803	1.027	1.070	1.176	6,150
- 6005V7	840	.843	.983	.820	9,250

$$2\sigma = \frac{p\ell\, t/2}{bt^3/12} = \frac{6p\ell}{bt^2}$$

$$= \frac{9p}{bt^2}$$

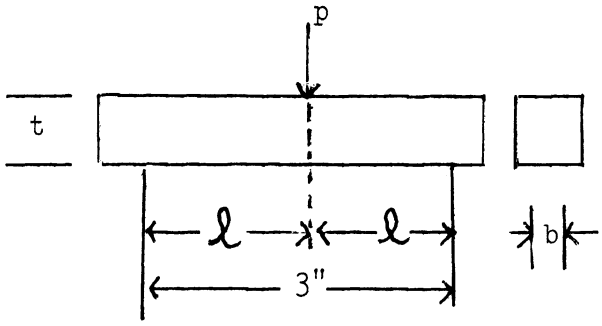

TABLE II

CALCULATED CRUSHING PRESSURES - (ρ) AT
FOUR DIFFERENT TEST CONDITIONS

Wheel	(A) Depth - d = 0.006 in. Feed - f = 0.125 ipr Area = 0.01675 sq in.			(B) d = 0.010 in. f = 0.052 ipr Area=0.00895 sq in.			(C) d = 0.006 in. f = 0.0125 ipr Area=0.001675 sq in.			(D) d = 0.0025 in. f = 0.052 ipr Area=0.00448 sq in.		
	(1) F_D	(2) F_W	(ρ)-psi	F_D	F_W	(ρ)-psi	F_D	F_W	( )-psi	F_D	F_W	-psi
48A60H5V6	86	122	7,300	61	86	9,600	13.5	19	11,300	23.5	33	7,400
- 60H8 -	52	73.5	4,400	34	48	5,400	5	7	4,200	9.7	13.7	3,050
- 60H12-	71	100	5,950	51	72	8,050	11	15.5	9,250	19	27	6,050
- 60K5 -	150	212	12,600	110	155	17,300	26	37	22,200	42.5	60	13,400
- 46H5 -	72	102	6,100	51	72	8,050	9.5	13.5	8,100	16.5	23.5	5,250
- 80H5 -	110	155	9,250	63.5	90	10,000	19.5	27.5	16,500	32	45	10,000
- 46I8 -	37	52.5	3,140	27.5	39	4,350	7.2	10	6,000	11	15.5	3,500
- 46J8 -	64	90	5,350	44.5	63	7,050	12.5	17.5	11,000	18.5	26	5,850
- 6005V7	255*	360	21,500	210*	300	33,600	58	82	49,000	70	99	20,000

(1) F_D = Force measured by the dynamometer in pounds.

(2) F_W = Actual force at the grinding wheel in pounds; $F_W = \sqrt{2}\, F_D$

*Extrapolated values.

A similar comparison of the pressures in columns B and D shows an increase in apparent pressure with increased depth whereas an increase in feed rate had the opposite effect. This stiffening effect with increased depth is related directly to behavior in acutal grinding as will be shown in a later section.

The pressures from Table II were plotted against the bending strengths in Table I. The resulting plots are shown both in cartesian and logarithmic coordinates in Figures 8-15 inclusive. There is reasonable consistency despite the fact that the calculated pressures cannot be the true fracture strengths in all cases. That the pressures do not correspond to the breaking strength is due to at least two factors. One is the presence a substantial elastic component in the measured forces. The other is that the number of grains available for contact at the surface of a grinding wheel is a sensitive function of the depth of cut. At test condition-D for example there may be only two grains being crushed at any one time but there are many more in the same cross-sectional area within the wheel. This latter factor explains why some of the crushing pressures in column-D of Table II drop below the corresponding strengths in bending.

The consistency which does appear in Figures 8-15 can be attributed to two things. First is the fact that the factors other than fracture strength which enter into the measured force on the dynamometer maintain an orderly relationship with the total force within each test condition. Secondly there should be some correlation with bending strength since all glasses fracture in tension regardless of the type of loading. More study will be needed before the manner in which all of the elastic factors combine with fracture strength to give the measured forces. Some promising evidence has come out of recent research on grinding itself, however.

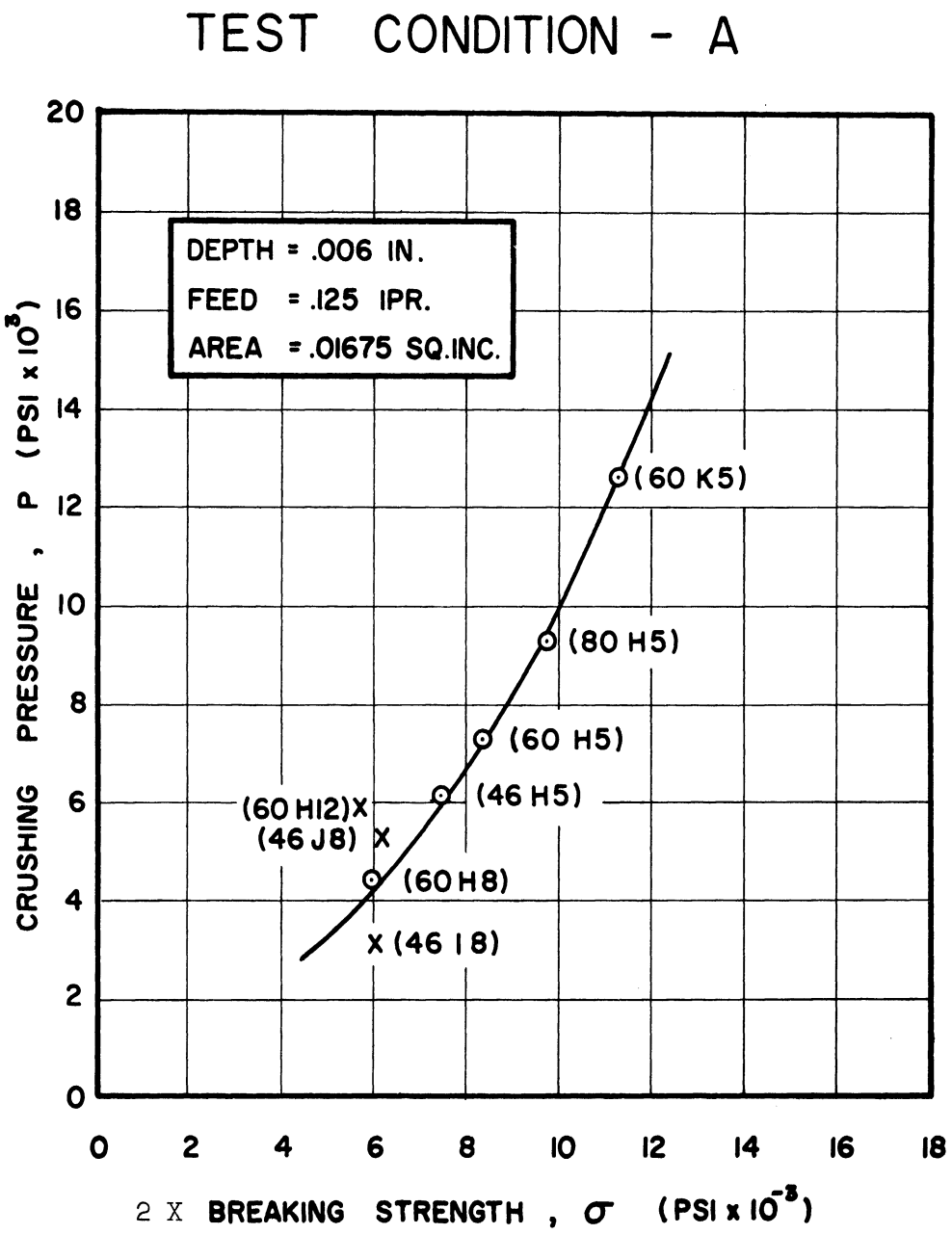

Figure 8

(Figures 8 through 15 - Calculated pressure in the crushing zone from Table II versus bending strengths from Table I. Test conditions A and C are for the same depth of cut but heavy and light feeds respectively. Similarly, conditions B and D are for constant feed and large and small depths respectively. Difference in calculated pressures for the same wheel reflect changes in elastic components.)

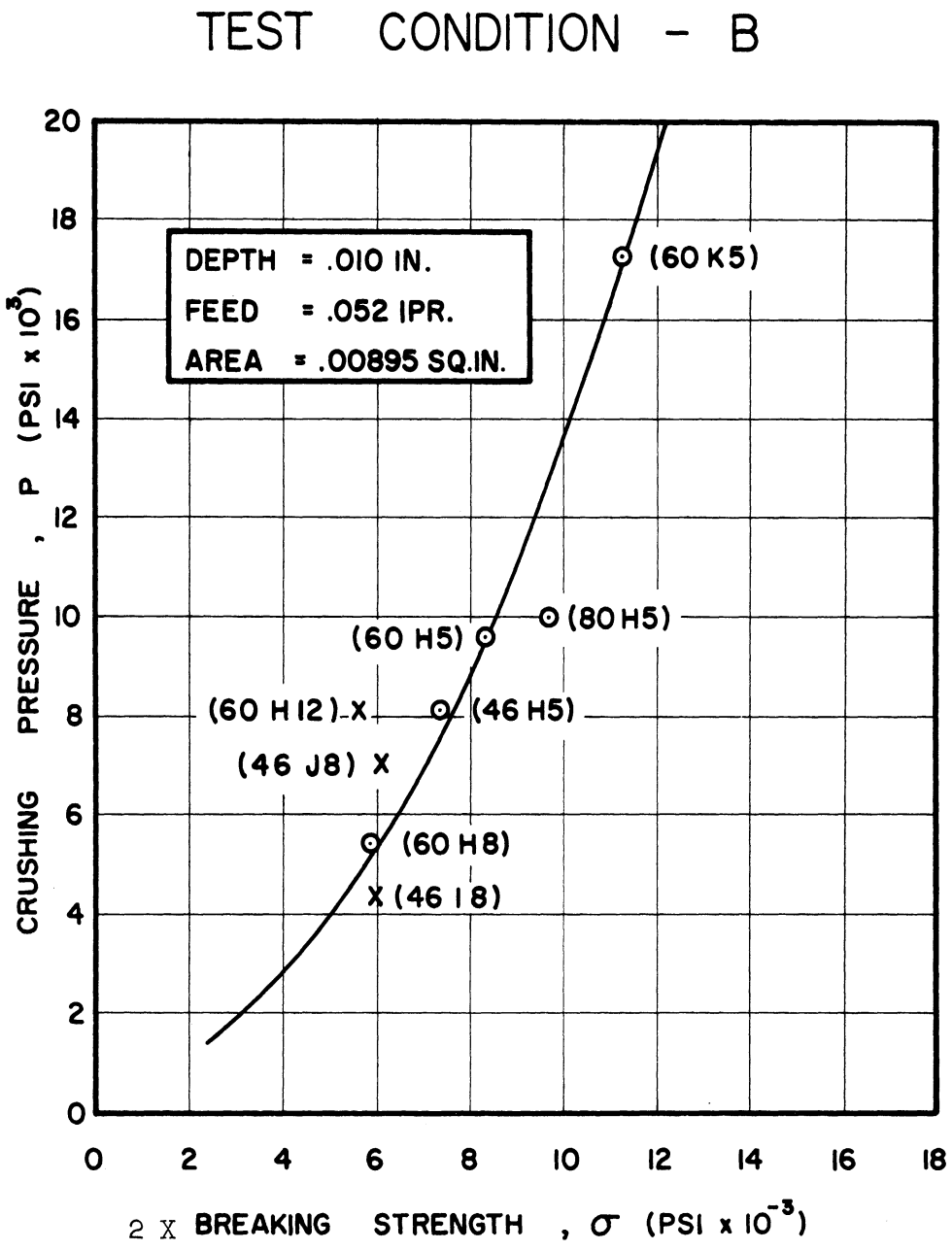
TEST CONDITION - B
DEPTH = .010 IN.
FEED = .052 IPR.
AREA = .00895 SQ.IN.
(60 K5)
(80 H5)
(60 H5)
(60 H12) X
(46 H5)
(46 J8) X
(60 H8)
X (46 18)
CRUSHING PRESSURE , P (PSI x 10^3)
2 X BREAKING STRENGTH , σ (PSI x 10^-3)
0
2
4
6
8
10
12
14
16
18
20

Figure 9

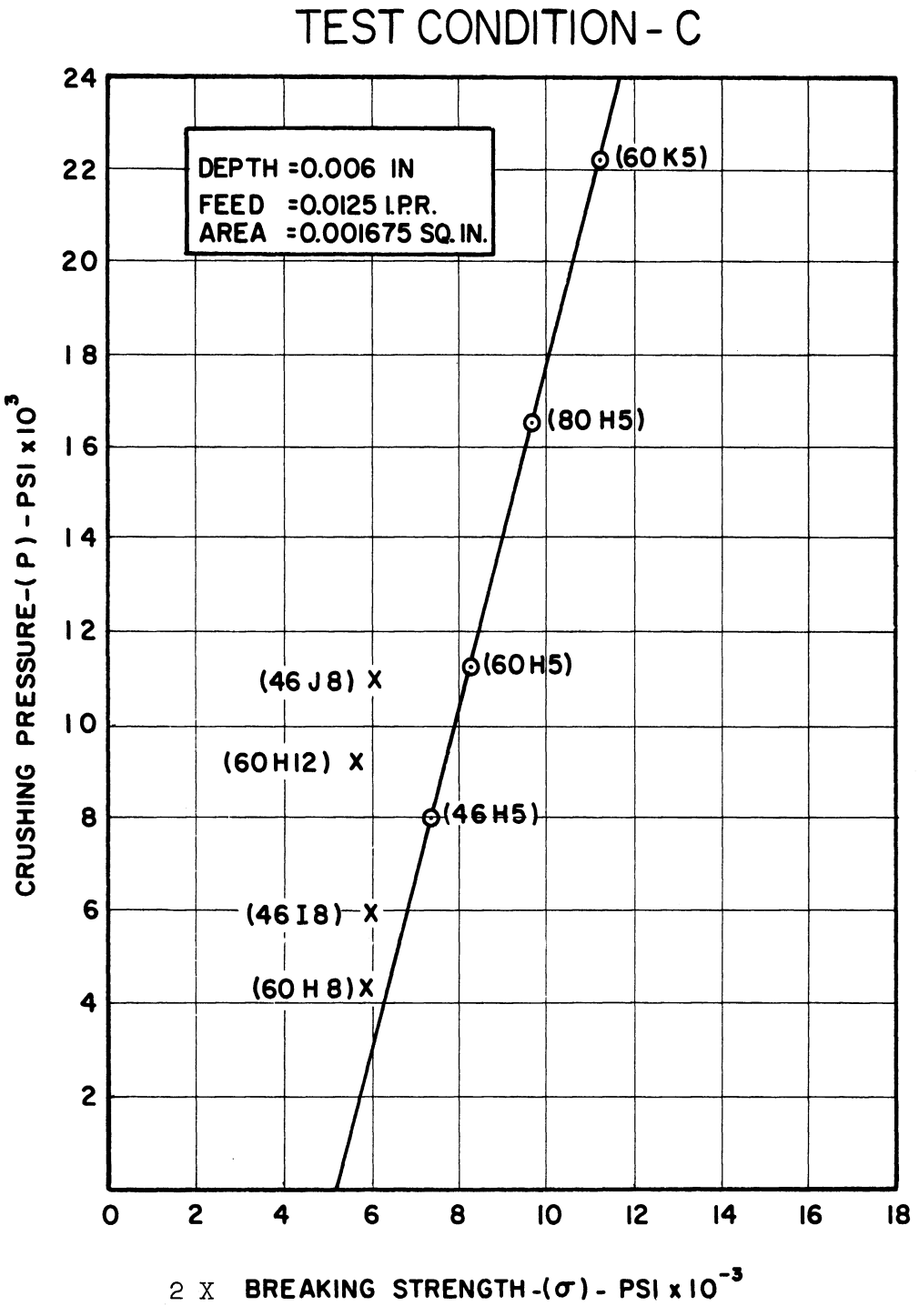
TEST CONDITION - C
DEPTH =0.006 IN
FEED =0.0125 I.P.R.
AREA =0.001675 SQ. IN.
(60 K5)
(80 H5)
(60 H5)
(46 H5)
(46 J 8) X
(60 H12) X
(46 I 8) X
(60 H 8) X
CRUSHING PRESSURE-(P) - PSI x 10³
2 X BREAKING STRENGTH-(σ) - PSI x 10⁻³
0
2
4
6
8
10
12
14
16
18
20
22
24

Figure 10

TEST CONDITION - D

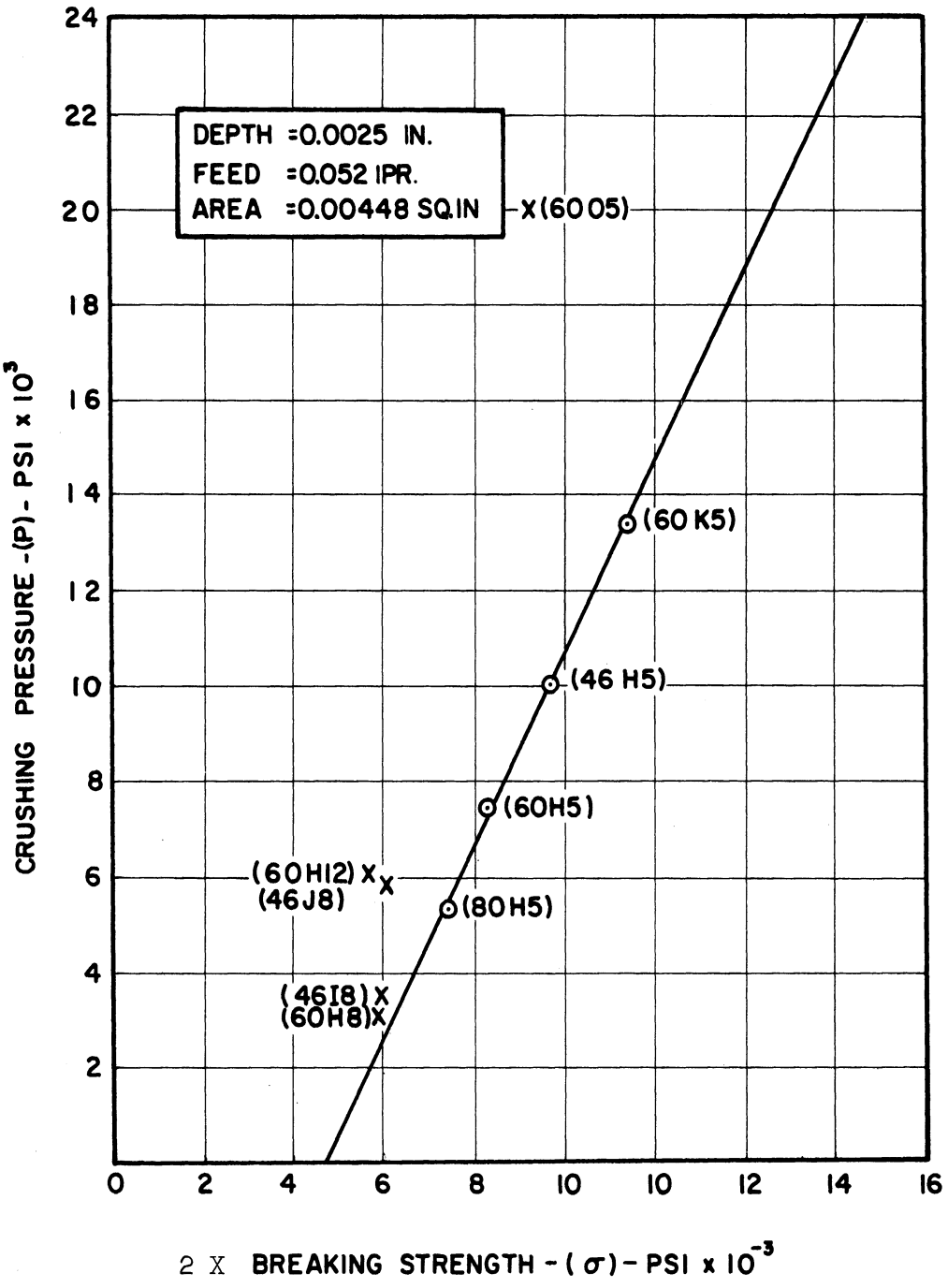

Figure 11

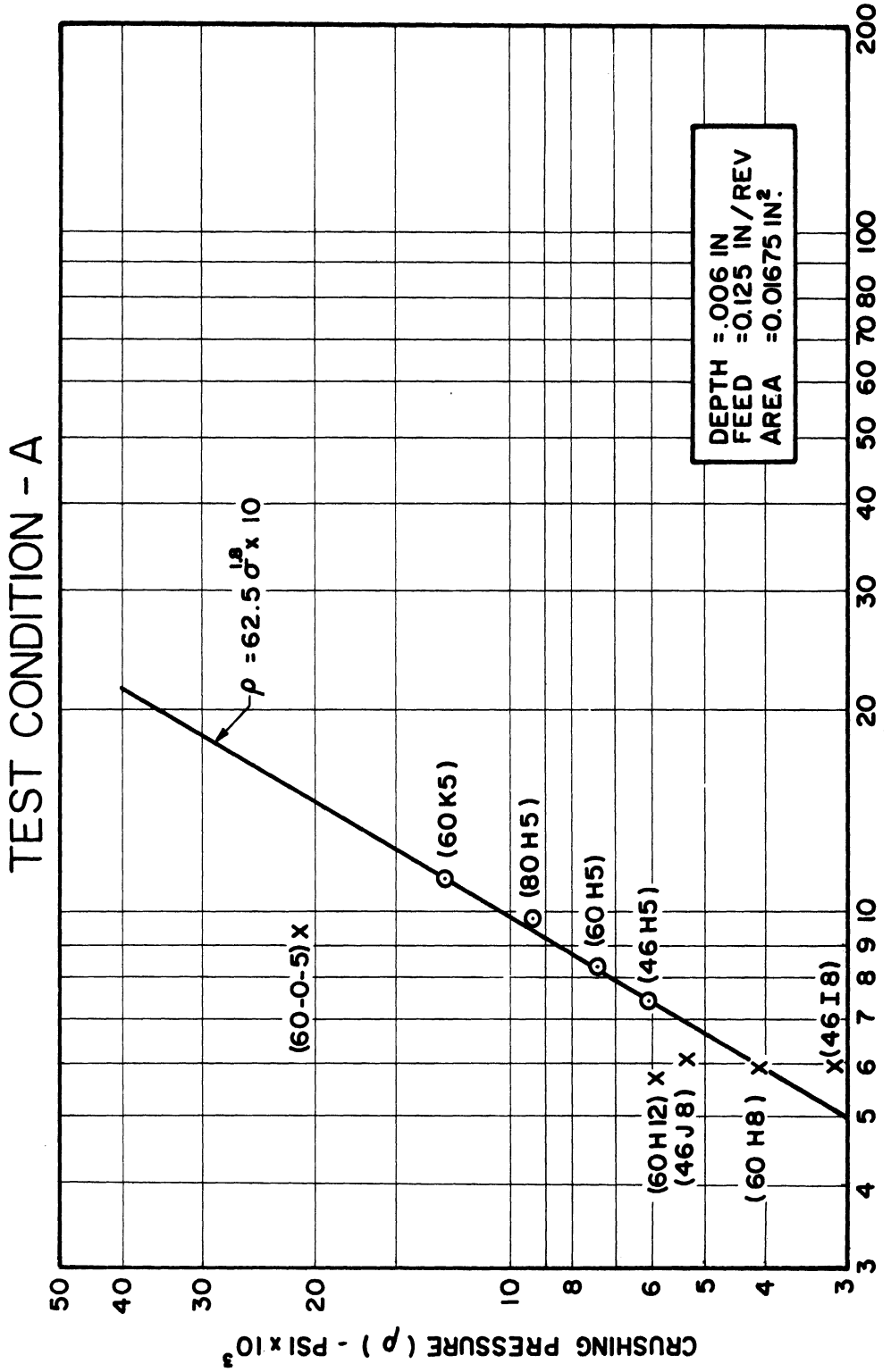

Errata: $\rho = 2220\ \sigma^{1.8} \times 10^{-6}$ Figure 12

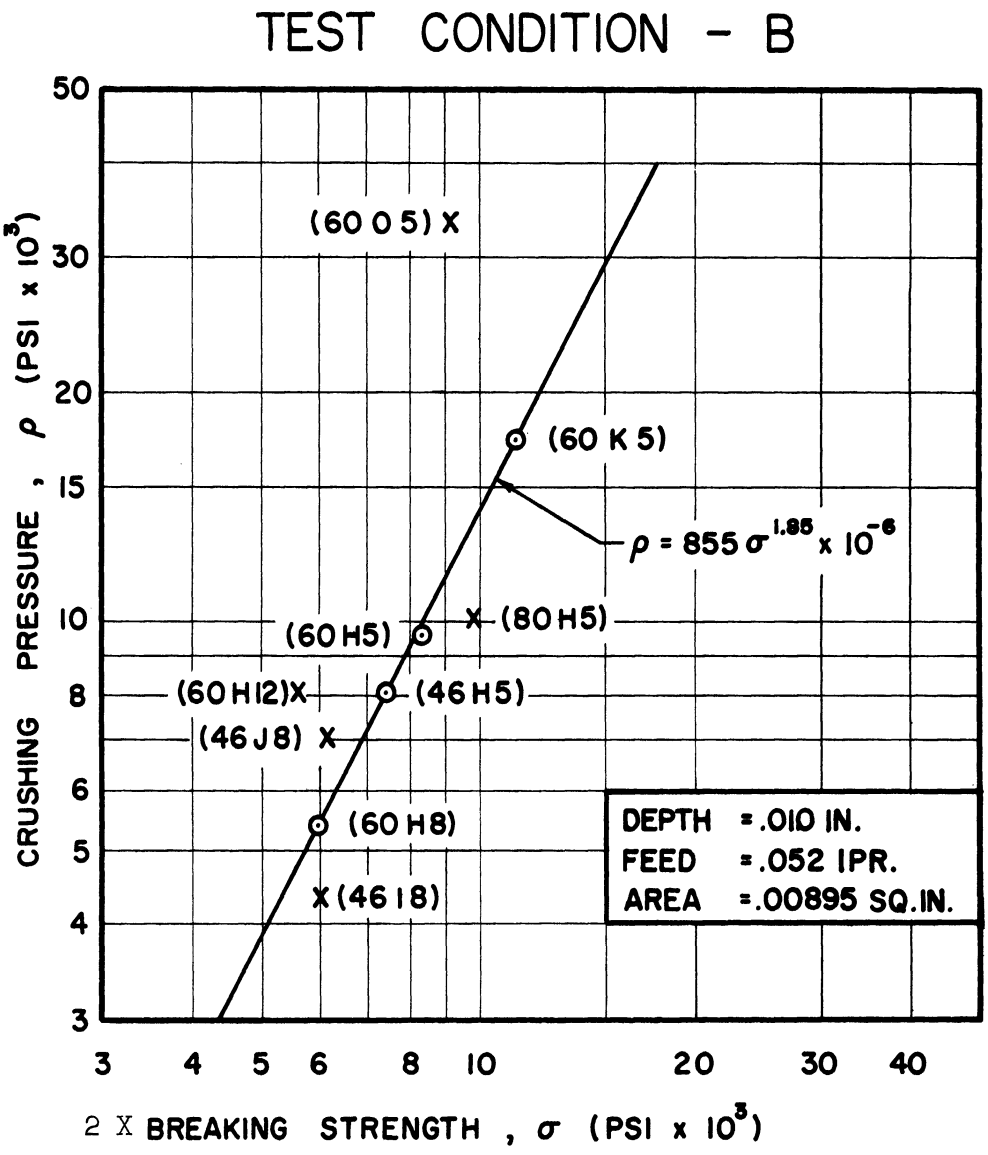

Errata: Figure 13

$\rho = 2020\ \sigma^{1.85} \times 10^{-6}$

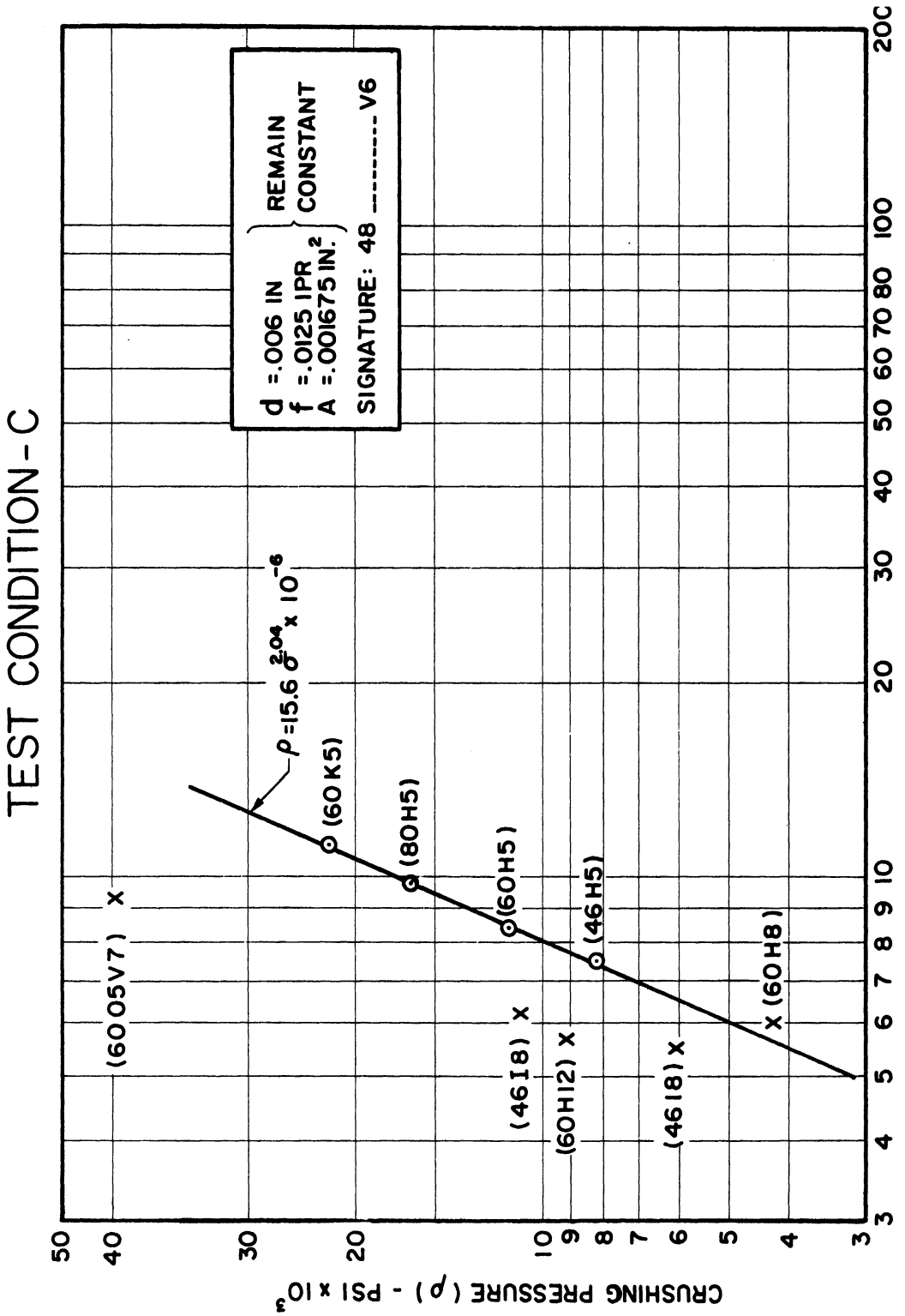

Figure 14

Errata: ρ = 22.4 $\sigma^{2.4}$ x 10^{-6}

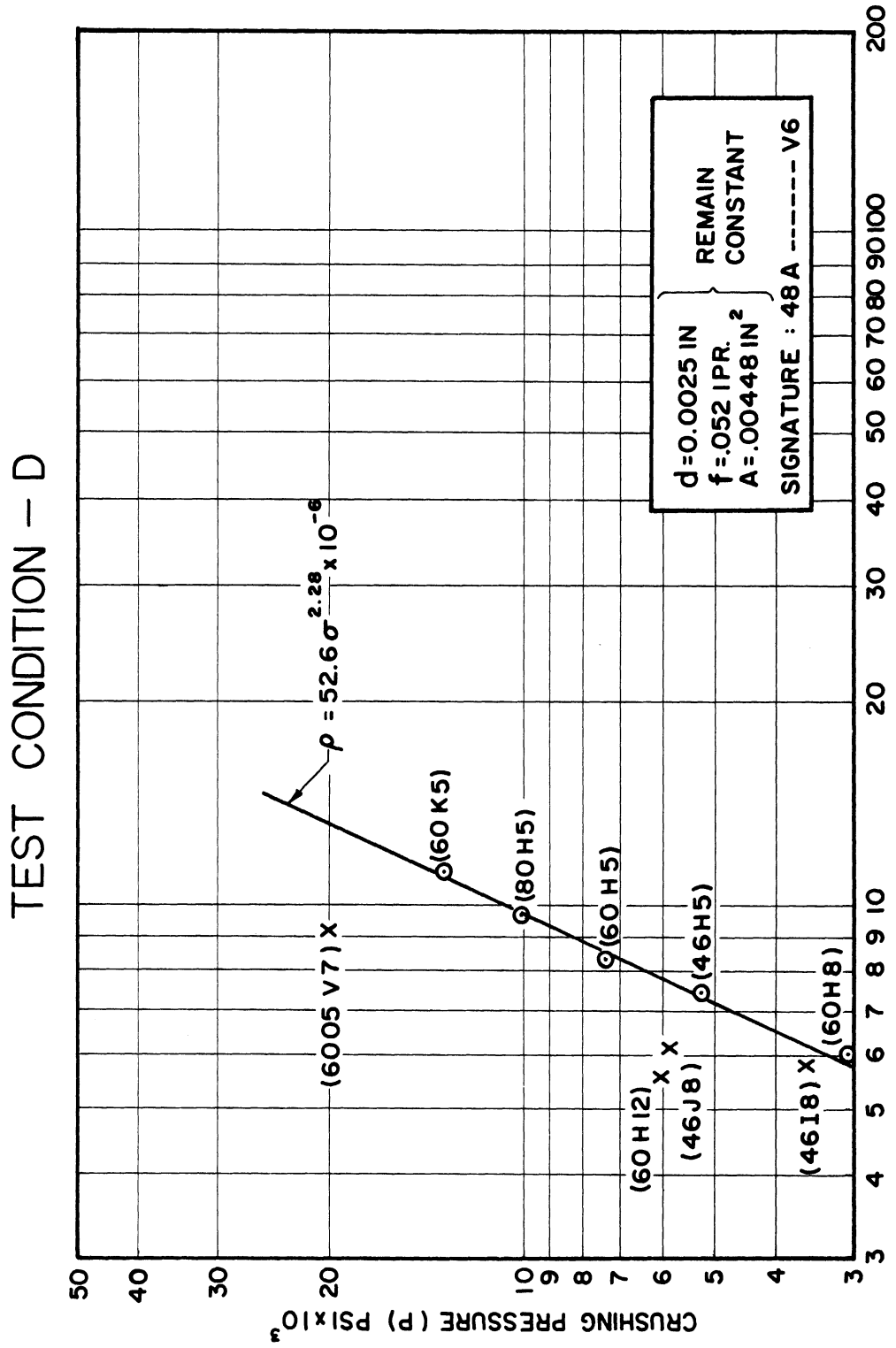

Errata: ρ = 38.8 σ2.28 x 10-6 Figure 15

Analysis and Interpretation

The fact that the data in Figures 4-7 is orderly and reproducible is gratifying in itself. However, the full significance and possible usefullness of such information depends on further analysis. It is obvious from visual observations that the mechanisms which control behavior in the crushing zone are quite complex and that they take place very rapidly.

An attempt has been made to illustrate some of these mechanisms in Figure 16 which is a front view of the contact zone. Three different sources of force components appear to be present. These components have been designated as crushing, elastic and packing components. An equation for measured force incorporating these components has been written but a review of the actual events occurring between the crushing wheel and the abrasive wheel is necessary before the individual terms appear to be relevant.

The proportions in Figure 16 represent a fine-grained wheel with a grit size of 120 or smaller. The cutter wall thickness is designated as $-t_c$ and the width of the area being crushed is designated by -f since it is determined by the feed rate in inches per revolution. The abrasive grains approach the crushing zone from the top of the figure.

The Crushing Component

Initial contact with the crushing wheel is elastic and force will build up with continued motion. If the interference is large the grain will either split or be broken away from the bond posts. On the other hand, initial contact may come only shortly before the tangent point

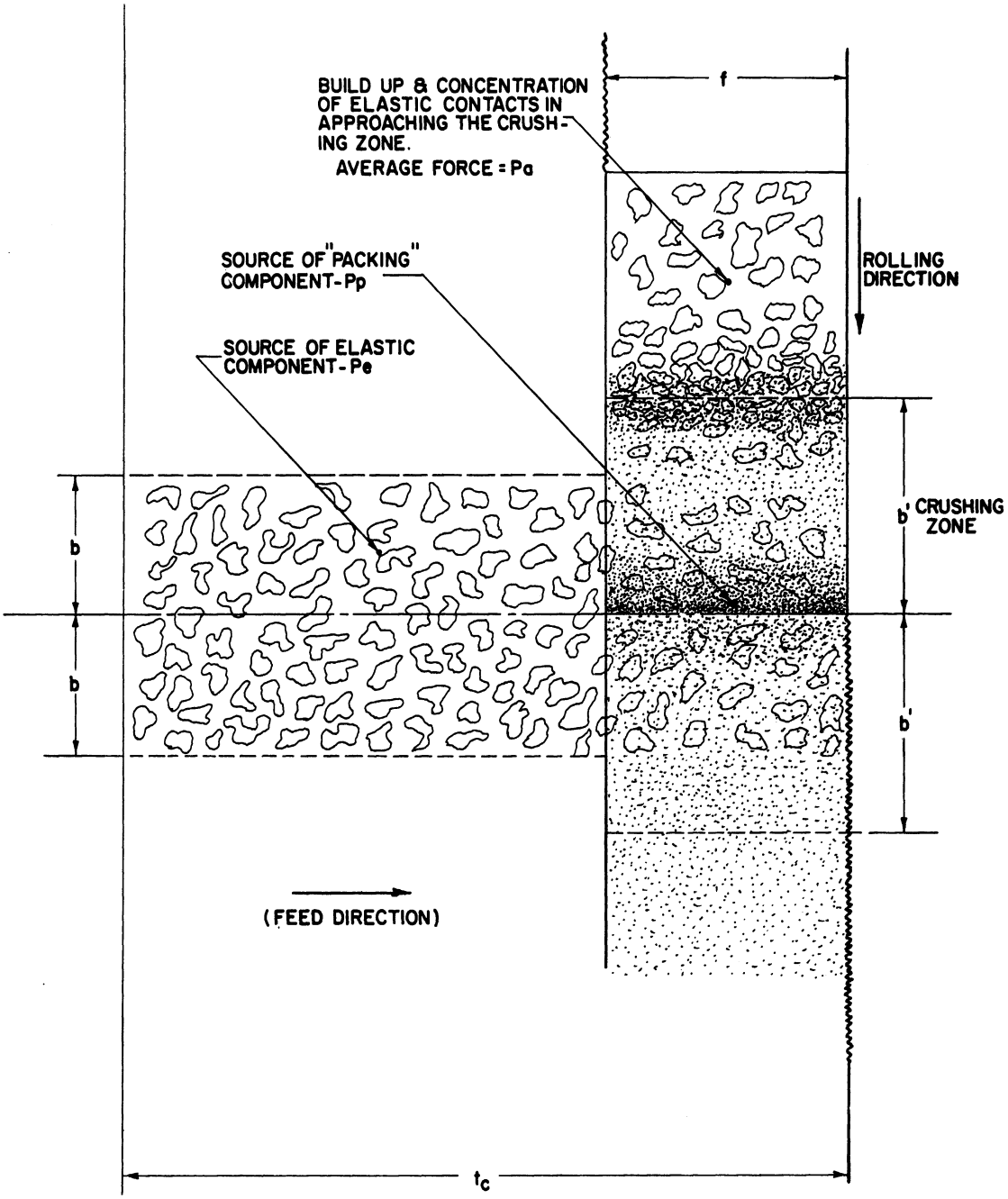

Figure 16. Front view of probable conditions in the contact zone between the crushing wheel and the grinding wheel. All grains make elastic contact since actual fracture is sudden and brittle in nature. All debris from crushing must pass between the wheels and can cause some packing at large depths of cut.

at the centerline in which case the contact conditions will remain elastic and the grain will pass on through the crushing zone without fracture taking place. Thus the force arising from this zone will be built-up elastically but this terminates in crushing for some grains if not for others. For this reason it has been called the crushing component. Its magnitude will be determined by strength properties and the number of grains in the zone. Thus the initial form of an expression for the crushing component could be

$$P_c = K_a N(\text{pounds}) \tag{1}$$

where:

K_a = some average force per grain in pounds

N = number of grains in contact.

Peklenik[1] found that the surface density in grains per unit of area increases exponentially according to the equation

$$K_z = Cd^n \tag{2}$$

where:

K_z = number of grains per unit area (Grain Concentration)

d = depth of cut in grinding (inches)

C = proportionality constant.

The data from which this equation was derived is shown in Figure 17 for four different grain sizes of vitrified aluminum oxide wheels. Appropriate values of -C and n as reported by Peklenik are summarized in Table III along with corresponding data on average grain diameter and center distance as reported by Maslov.[2]

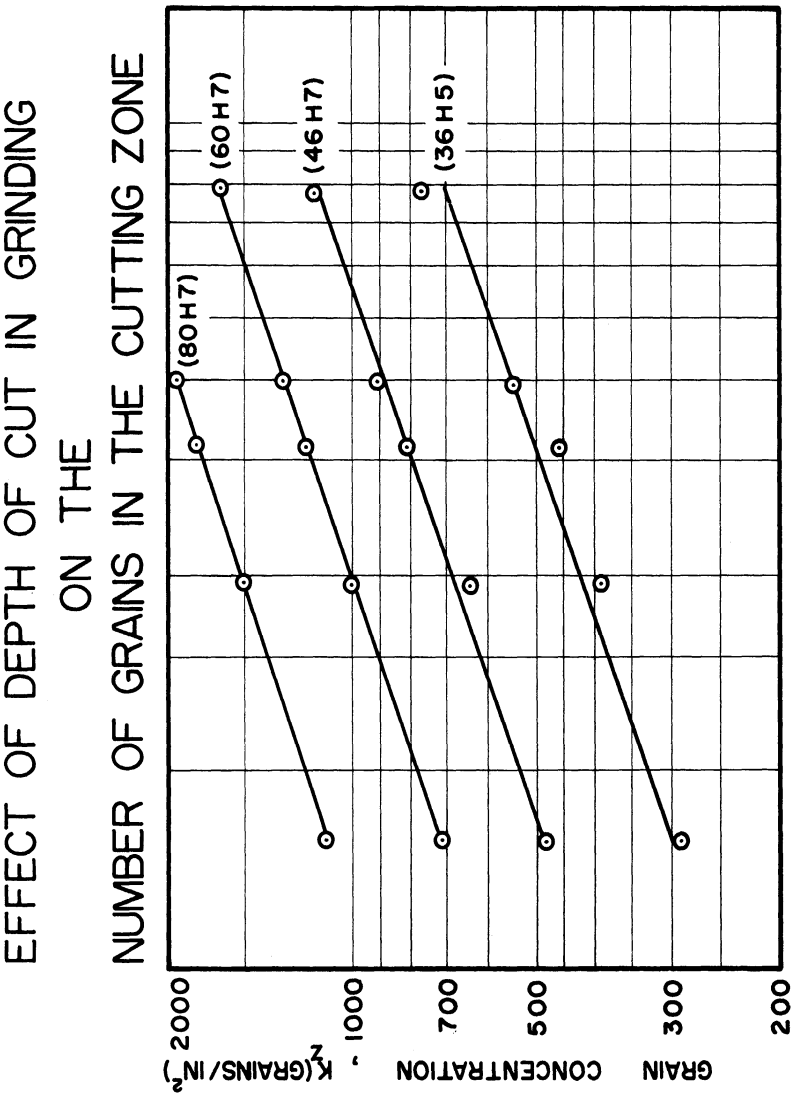

Figure 17. Shows the increase in the number of abrasive grains per unit area in the cutting zone as the depth of cut in actual grinding is increased. The increase in pressure at greater depths causes the higher grains to be deflected elastically toward the center thus producing a larger concentration of grains. Results were obtained for surface grinding of a medium carbon steel with cup wheels. (From the dissertation of J. Peklenik, Reference 1)

TABLE III

GRAIN CONSTANTS AND CONCENTRATION COEFFICIENTS

Grit No.	$K = Cd^n$ (a)		Average Diameter-in. (b)	Average Center Distance-λ(in.) (b)
	C	n		
36H5	1520	0.368	0.0212	0.0187
46H7	2300	0.370	0.0141	0.0149
60H7	3520	0.370	0.0092	0.0103
80H7	5735	0.365	0.0070	0.0092

(a) According to Peklenik[1]

(b) According to Maslov[2]

Since the individual grain contacts are elastic all the way up to fracture, it is reasonable to expect that Equation (2) will be applicable to some degree in crushing as well as in actual grinding itself. On this basis Equations (1), (2) can be combined with the equation for the area of the crushing zone (B-5)* to give

$$P_c = \sqrt{3}\, K_a C f d^{0.5+n} \qquad (3)$$

where:

P_c = crushing component - pounds

K_a = average force per grain - pounds

C = proportionality constant from Equation (2)

f = feed rate - ipr

d = depth of crushing - inches

n = exponent from Equation (2).

* The derivation of this equation is given in the Appendix, part II.

When the system, including the dynamometer, is relatively rigid and the depth of cut is not very large, the actual depth of crushing may be deep enough so that there will be no contact on the return pass. This would indicate that the elastic component - P_e and the packing component P_p as suggested in Figure 16 did not exist at these conditions in which case the total load on the dynamometer would be represented by Equation (3).

Experimentally, the above set of conditions was satisfied in the tests on the 48A60H8V6 wheel for which the results are plotted in Figure 5. It will be noted in Figure 5 as well as in Table IV that the measured force for this wheel is expressed by the equation

$$F_D = Kf^{1.0}d^{.89} \quad .$$

It is interesting to note the qualitative similarity between this result and Equation (3) when the appropriate values of (n) and (C) from Table III are inserted. In this case, Equation (3) becomes

$$P_c = 6100\ K_a f d^{.87} \quad .$$

It will be noted further in Table IV that the exponents for the 48A60H8V6 wheel were the largest. This means that some combination of the elastic and packing components were present in the measured forces for the other wheels. This possibility was substantiated by varying amounts of interference and further crushing when the cutter was traversed back over the abrasive wheels without additional infeed.

TABLE IV

SUMMARY OF CRUSHING FORCE EQUATIONS*

$(F_D = Kf^x d^y)$*

Wheel	K	Y	X
48A60H5V6	13,700	.67	.79
-60H8-	39,000	.89	1.0
-60H12-	16,000	.73	.81
-60K5-	24,600	.68	.77
-46H5-	27,000	.80	.88
-80H5-	10,700	.59	.75
-46I8-	4,350	.65	.70
-46J8-	6,550	.63	.70
-6005V7	70,000	.79	.71

*Dynamometer Force = $F_D = Kf^x d^y$

where: f = feed (inches per revolution)

d = depth crushed from wheel surface (inches)

K = proportionality constant

The Elastic Component - P_e

An expression for the elastic component P_e as designated in Figure 16 is difficult to derive by direct calculation since the geometry of individual grain contacts is not known well enough yet to permit even statistical treatment of the problem. However, the events leading up to crushing are relatively simple and they demonstrate that an elastic component must exist.

This was deduced from the following observations.

1) There are very few grains in contact with the crushing wheel at any one instant even at relatively heavy cuts.
2) The stiffness of the entire system including the dynamometer is substantially less than that of individual grains in the abrasive wheel
3) The deflection of the system in building up a force sufficient for crushing may be several times the diameter of the grains which are broken out.

At very small depths and light loads, the crushing wheel will simply ride up and down over the high spots on the surface causing oscillations in the force record produced by the dynamometer. With very low system rigidity this would continue to prevail even at large system deflections. As the system is stiffened up, the force variations resulting from riding up and down over the high spots will increase with the result that some of the high spots or grains will be crushed. The crushing permits the load to relax but not all the way to zero necessarily.

For example, the laboratory test set-up had a system rigidity of 7000 pounds which caused a total deflection of 0.010 inches when the

required crushing load was 70 pounds. This load was required to crush the 48A80H5 wheel at a depth of 0.006 in. and a feed rate of 0.070 ipr. Obviously the wheel could ride up and down no more than the depth of cut so that the absolute minimum elastic component would be 28 pounds. It is more likely that the oscillatory movement of the crushing wheel is no more than the radius of a grain or at most, half the average center distance. Table III shows for an 80 Grit wheel this distance could be from 0.0035 to 0.005 inches. It can be expected that harder grade wheels with lower porosity would further reduce this distance. Therefore, the combination of the elastic and crushing components could be expressed as

$$F = \sqrt{3}\, K_a C f d^{0.5+n} - \phi_1(K_s\lambda,\rho,d,f)\left(\frac{1 + \sin\omega t}{2}\right) + \phi_2(t_c,\sigma_o,k_1 + k_2,r)\left(\frac{N + \sin\omega t}{N + 1}\right) \qquad (4)$$

where:

K_s = modulus of elasticity of the system

λ = average center distance between grains

ρ = fraction porosity (e.g., $\rho = .45 = 45\%$ porosity)

d = depth of cut

t_c = wall thickness or width of crushing wheel

k_1+k_2 = elastic constants of both wheels (see Appendix IV)

r = average radius of abrasive grains

t = time

ω = function of surface velocity and grain spacing at the surface

ϕ_1,ϕ_2 = unresolved functions

σ_o = average fracture stress

The "Packing" Component - P_p

The packing component will be discussed before trying to interpret Equation (4). All of the debris crushed from the surface of the wheel must pass between the two wheels so that combinations of low porosity and large depth of cut can cause some further interference between the wheels and consequently some additional load. The added load will be a product of the added system deflection and the system modulus K_s.

It can be shown that this load, that is, the packing component can be expressed as

$$P_p = \phi_3 \left\{K_s\left[\left(\frac{fd}{f+a\lambda}\right)(1-\rho) - \rho b\lambda\right]\right\} \left(\frac{N+\sin\omega t}{N+1}\right) \qquad (5)$$

where:

a,b = multipliers of λ

ϕ_3 = unresolved function.

The packing has a far greater effect in the contact zone than would be indicated by Equation (5) since it reduces or takes over at least part of the elastic load represented by the third term of Equation (4). This component is essentially elastic also but it is confined to the crushing zone and has little practical significance except that excessive amounts of packing would alter the shape of the surface of the crushing wheel and reduce sensitivity of the process to the important properties represented in the so-called elastic component. Practically then, the packing phenomenon establishes upper limits on size of cut where the process is to be used for investigation and evaluation of the effective hardness of bonded abrasives.

The Total Force - F

The total indicated force is represented in a general equation by adding Equation (5) to Equation (4) to give

$$F = \sqrt{3}\, K_a C f d^{0.5+n} - \phi_1(K_s\ \lambda,\rho,d,f)\left(\frac{1+\sin\omega t}{2}\right) + \left(\frac{N+\sin\omega t}{N+1}\right)[\phi_2(t_c,\sigma_o,k_1+k_2,r)] + \left(\frac{N+\sin\omega t}{N+1}\right)[\phi_3 K_s\{(\frac{fd}{f+a\lambda})(1-\rho) - \rho b\lambda\}] \qquad (6)$$

The terms $(\frac{1+\sin\omega t}{2})$ and $(\frac{N+\sin\omega t}{N+1})$ make the last three terms oscillatory in behavior. The term $(\frac{1+\sin\omega t}{2})$ oscillates between zero and unity. The other term oscillates between unity and some number greater than zero but less than one. Thus the elastic terms will not be reduced to zero when N is greater than one. Studies aimed at resolving the unknowns in this equation are being carried out and will be the subject of further reports.

Testing the Equation

Equation (6) can be evaluated qualitatively only until further studies are completed. The basis for evaluation is the slopes of the lines in logarithmic coordinates. The addition of a constant number to an existing straight line in double-logarithmic coordinates gives another straight line of flatter slope.

It has already been shown that the slopes can approach those in the first term when a wheel is relatively soft. On the other hand, if the elastic component exists outside the crushing zone then it will never completely disappear and the resulting slopes will all be flatter than the exponents of feed and depth in the first term.

It would appear that the first two terms of Equation (6) are dominant since the magnitudes of the elastic terms are primarily results of these terms rather than being independent causes. Consequently the behaviour of the equation as it relates to grain size and porosity will be determined primarily by the second term.

Grain size effect can be seen in Figure 4 for grits Nos. 46, 60, and 80. The nature of the second term of the force equation indicates that smaller grain sizes will cause a proportially large elastic force which in turn produces the progressively flatter slopes in this group.

Nominally, the porosity varies according to certain tabular specifications like those reported by Ljubomudrov[3] in Table V. It will be noted that the porosity by volume varies only between grades and that the proportional change between grades is almost negligible. Consequently, the ratio of the second term to the first should remain substantially constant between grades and the slopes should be approximately equal. This was the case for the two sets of lines in Figures 6 and 7.

The effect of structure is much more complex and requires further study. The H12 structure shown in Figure 6 is not comparable to the other two since the porosity is not uniformly distributed; it is characterized by blocky aggregates of grains and occasional large pores.

Further study of the significance of slope variations is represented in Figures 18, 19 and 20 inclusive. The lines represent many test on the same grinding wheel. The maximum, minimum and average forces were read off the charts and plotted as separate sets of lines. Further, the resulting slopes were plotted against the corresponding values of constant depths and feeds.

TABLE V

STANDARD PROPORTIONS OF ABRASIVE, BOND AND POROSITY*

Norton Hardness Scale		E	F	G	H	I	J	K	L	M	N	O	P	Q	R	S	T	V
Structure No.	Grain Volume in %	Volume in Percent																
		49.5	48	46.5	45	43.5	42	40.5	39	37.5	36	34.5	33	31.5	30	28.5	27	25.5
		Bond Volume in Percent																
0	62	--	--	--	--	--	--	--	--	0.5	2	3.5	5	6.5	8	9.5	11	12.5
1	60	--	--	--	--	--	--	--	1	2.5	4	5.5	7	8.5	10	11.5	13	14.5
2	58	--	--	--	--	--	--	1.5	3	4.5	6	7.5	9	10.5	12	13.5	15	16.5
3	56	--	--	--	--	0.5	2	3.5	5	6.5	8	9.5	11	12.5	14	15.5	17	18.5
4	54	--	--	--	1	2.5	4	5.5	7	8.5	10	11.5	13	14.5	16	17.5	19	20.5
5	52	--	--	1.5	3	4.5	6	7.5	9	10.5	12	13.5	15	16.5	18	19.5	21	22.5
6	50	0.5	2	3.5	5	6.5	8	9.5	11	12.5	14	15.5	17	18.5	20	21.5	23	24.5
7	48	2.5	4	5.5	7	8.5	10	11.5	13	14.5	16	17.5	19	20.5	22	23.5	25	26.5
8	46	4.5	6	7.5	9	10.5	12	13.5	15	16.5	18	19.5	21	22.5	24	25.5	27	28.5
9	44	6.5	8	9.5	11	12.5	14	15.5	17	18.5	20	21.5q	23	24.5	26	27.5	29	30.5
10	42	8.5	10	11.5	13	14.5	16	17.5	19	20.5	22	23.5	25	26.5	28	29.5	31	32.5
11	40	10.5	12	13.5	15	16.5	18	19.5	21	22.5	24	25.5	27	28.5	30	31.5	33	34.5
12	38	12.5	14	15.5	17	18.5	20	21.5	23	24.5	26	27.5	29	30.5	32	33.5	35	36.5

*As reported by V.J. Ljubomudrov (Bibliography No.).

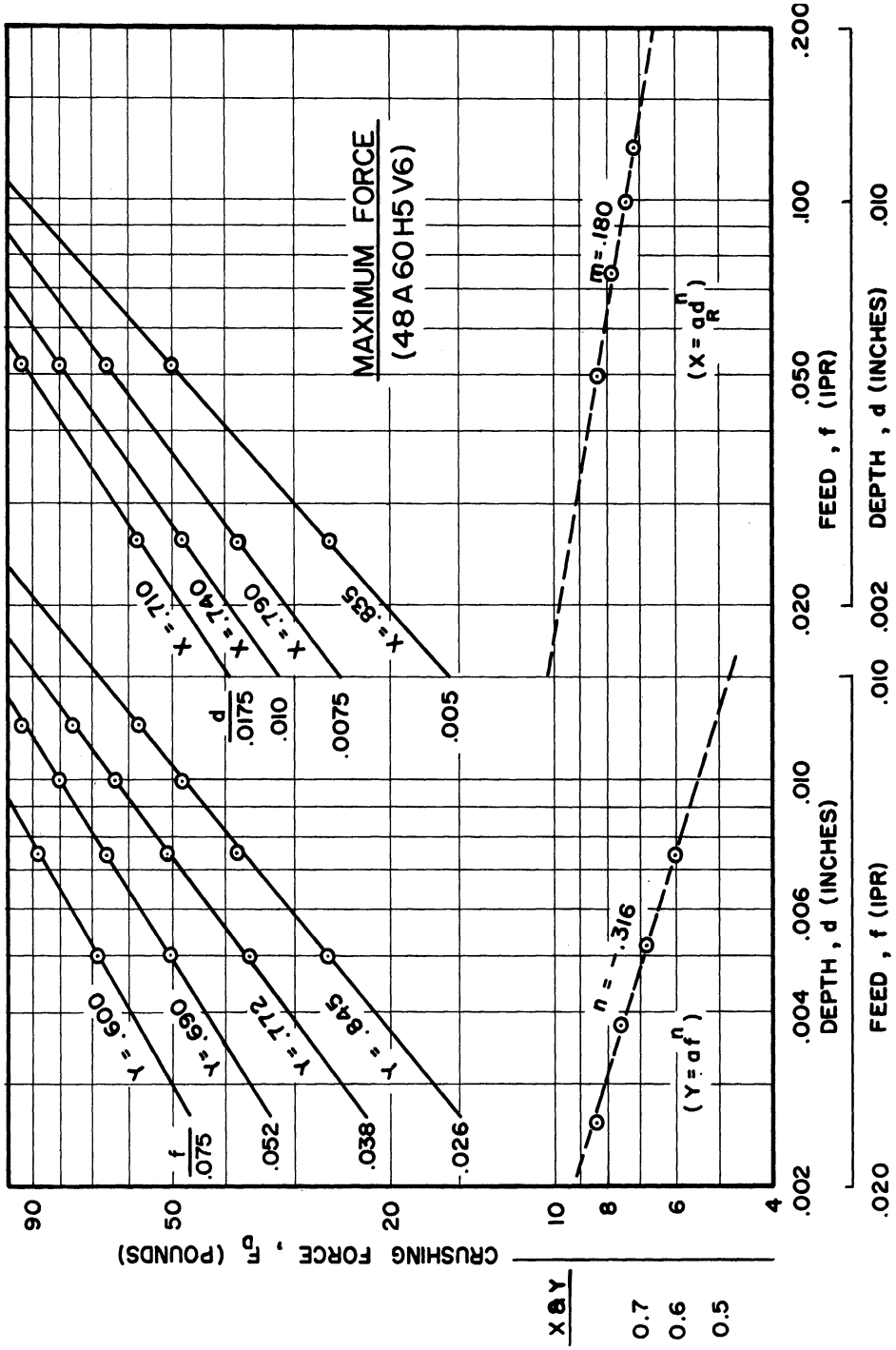

Figure 18

(Figures 18 through 20 - Crushing force for variable depth and feed at four different values of constant feed and four different values of constant depth for the same abrasive wheel. Note orderly progression of slope changes. All tests carried out at 319 rpm.)

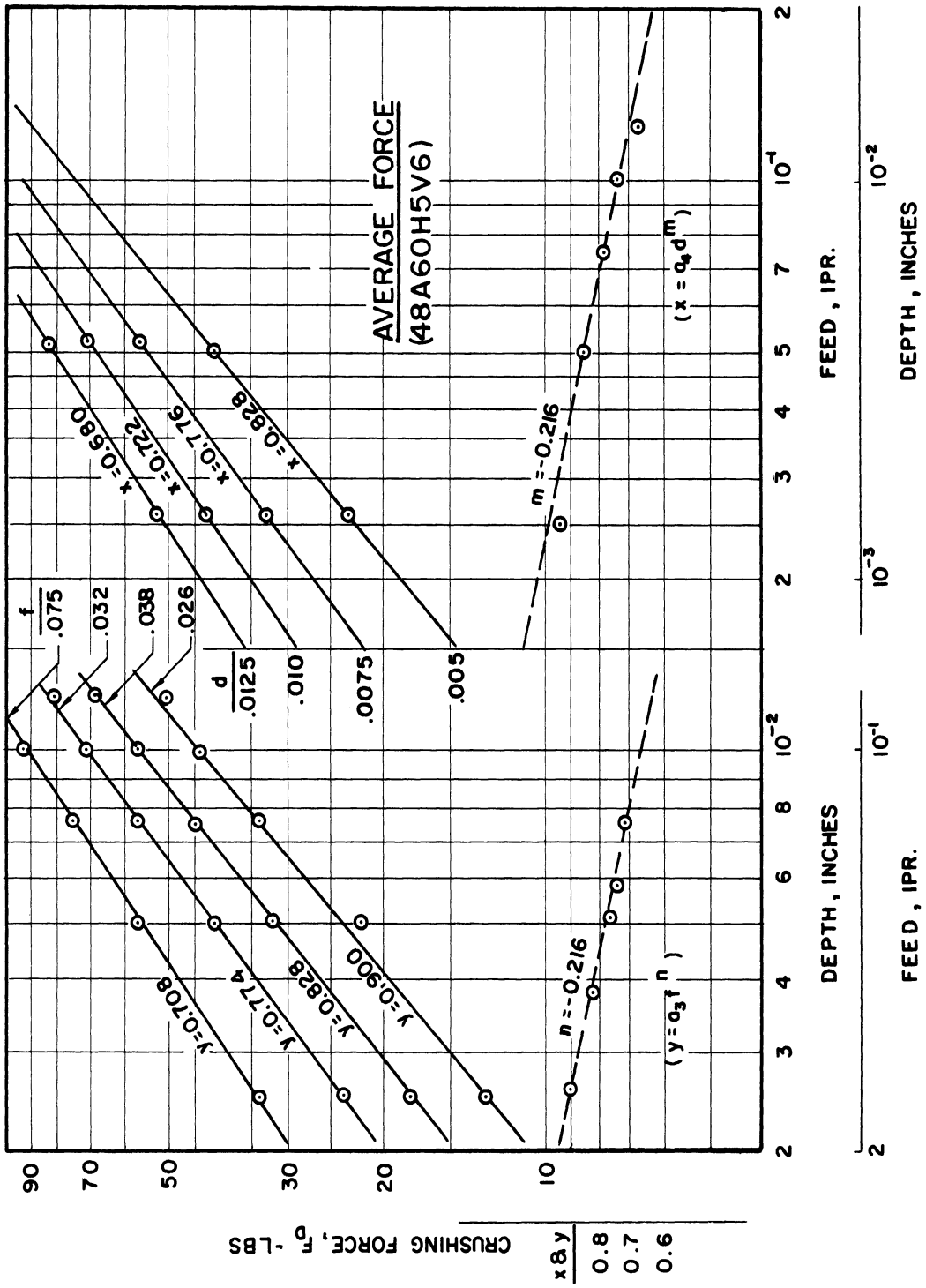
AVERAGE FORCE
(48A60H5V6)
CRUSHING FORCE, F_G -LBS
x&y
0.8
0.7
0.6
f
.075
.032
.038
.026
d
.0125
.010
.0075
.005
y=0.708
y=0.774
y=0.828
y=0.900
x=0.680
x=0.726
x=0.776
x=0.828
n=-0.216
($y=a_3 f^n$)
m=-0.216
($x=a_4 d^m$)
FEED, IPR.
DEPTH, INCHES
DEPTH, INCHES
FEED, IPR.

Figure 19

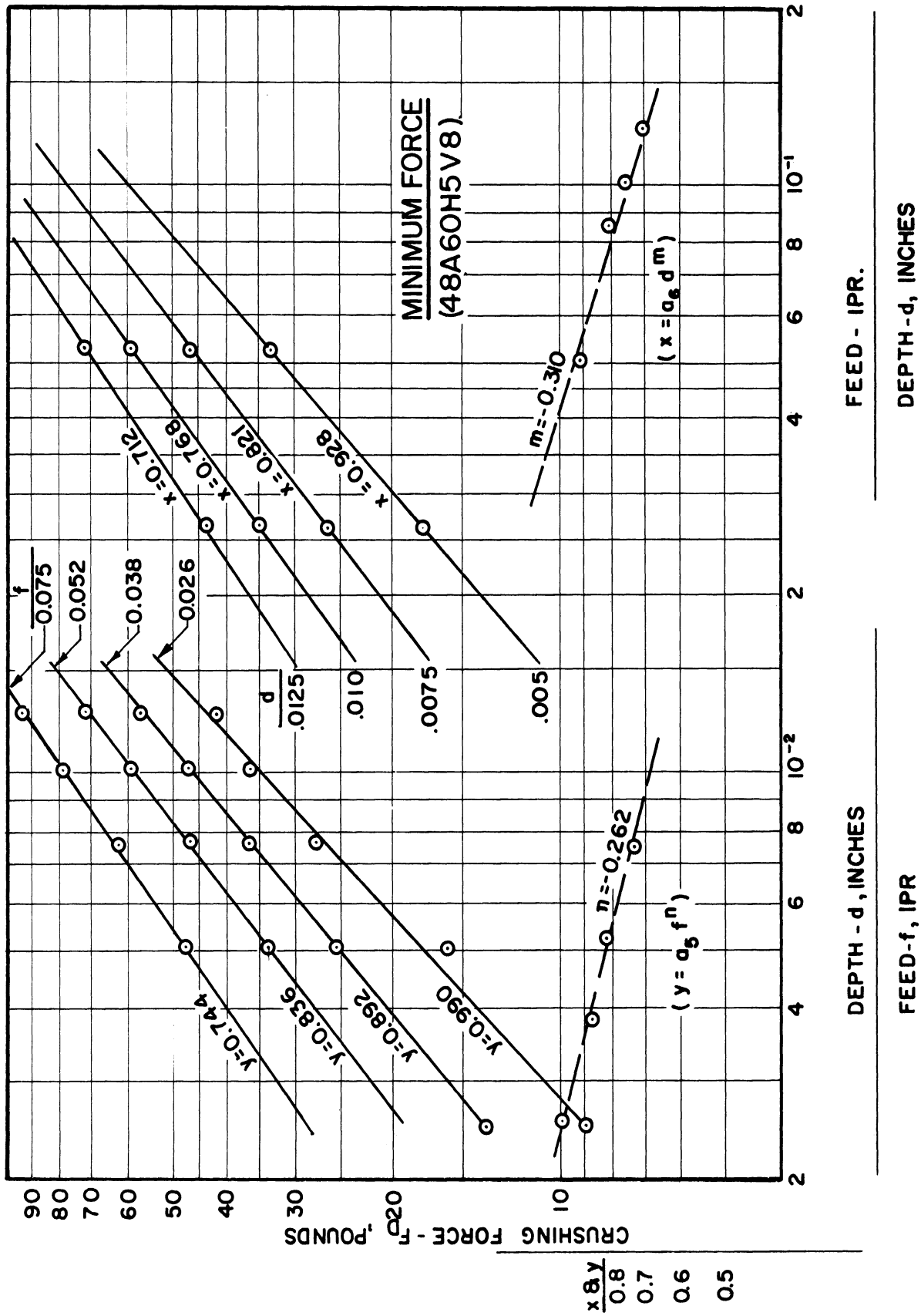
MINIMUM FORCE
(48A60H5V8)
CRUSHING FORCE - F_c, POUNDS
DEPTH - d, INCHES
FEED - IPR.
DEPTH - d, INCHES
FEED - f, IPR
$x = a_6 d^m$
$y = a_5 f^n$
m = -0.310
n = -0.262
x = 0.928
x = 0.821
x = 0.768
x = 0.712
y = 0.990
y = 0.892
y = 0.836
y = 0.744
f: 0.075, 0.052, 0.038, 0.026
d: .0125, .010, .0075, .005

Figure 20

Undoubtedly some of the slope changes are a load-level effect although there are some indications that it is also related to the actual number of grains in contact in the crushing zone and to some change in the exponent-n itself as the size of cut is increased. Peklenik's experience with finer grain sizes is another indication of this possibility. In any event, the orderly progression of slope changes shows promise for another fruitful area of research.

In summary, it should be pointed out that Equation (6) for the total force is tentative and to some extent also speculative. The number of terms may change and certainly their form will change as more information is evolved. However, it is already reasonably well established that this approach to evaluating the hardness of grinding wheels does incorporate elastic behavior and that it produces measurements which must reflect substantially the same properties which Peklenik and others have found to be important in actual grinding.

Application

The orderliness and repeatability of the dynamometer force measurements and the origin of the force components suggest several possible applications and uses. One of the obvious applications is for inspection and quality control of grinding wheels where the process has already been in use for a few months.

Quality Control

Figure 21 is a reproduction of the original test record of a 24 x 7 x 12 vitrified wheel produced before this method of inspection was put into operation. The customer returned the wheel claiming that

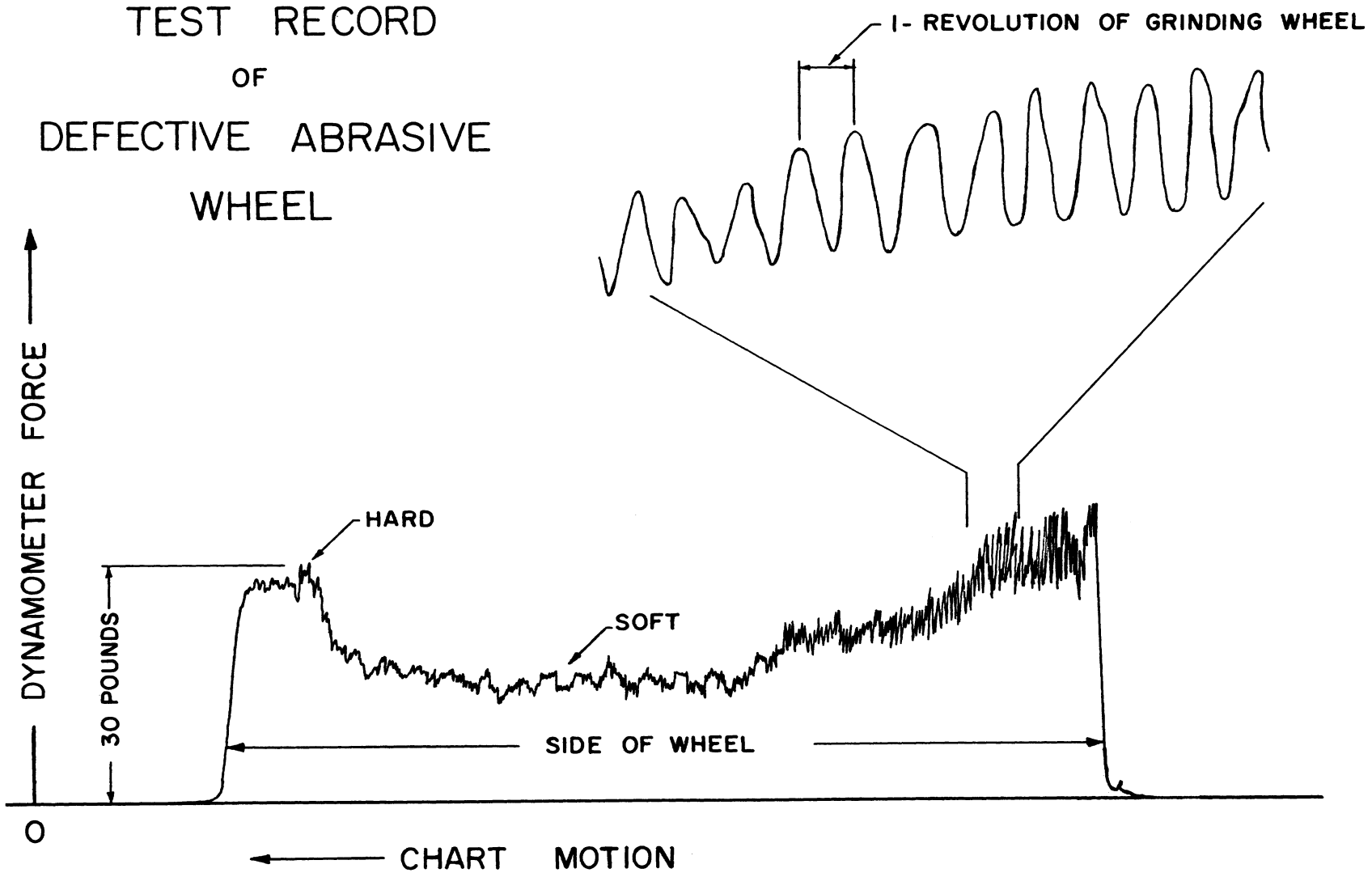

Figure 21. A reproduction of actual test record for the circumference of a defective grinding wheel. Sides are hard and middle is soft. Right side shows variation of 20-25% in hardness around circumference. Time for test traverse = 23 seconds.

it was defective. The test record substantiates the complaint. It is hard on the sides and soft in the middle in a ratio of about two to one. Furthermore, the right hand side shows a variation in hardness of from 20 to 25% around the circumference of the wheel.

The procedure is fast and economical. A single pass across this wheel required only 23 seconds. New cutter wheels are used from an original diameter of 3 inches down to 2-3/4 inches and then transferred to the main cutter spindle where they are used up. This results in a cutter cost of about one cent per day for inspection in contrast to more expensive diamond and carbide tools used in some other processes. More important than low cutter cost is the fact that cutter wear is uniform so that it always provides the same shape and size of contact surface. This is very important for the maintenance of consistency in a test of this type.

An Industrial Standard

This study also has indicated the feasibility of establishing industrial standards for grinding wheel hardness. With this objective in mind a brief exploratory study was made with a two-pass procedure which makes it possible to assign a dimensionless number for wheel hardness. Since this method of testing produces force data, then a dimensionless number can be obtained through a ratio of forces.

Figure 22 shows the dynamometer forces obtained in laboratory investigation of a two-pass procedure. In this approach the cutter is adjusted for a particular depth and feed rate and then fed across the face of the grinding wheel and the resulting force is measured. Then it

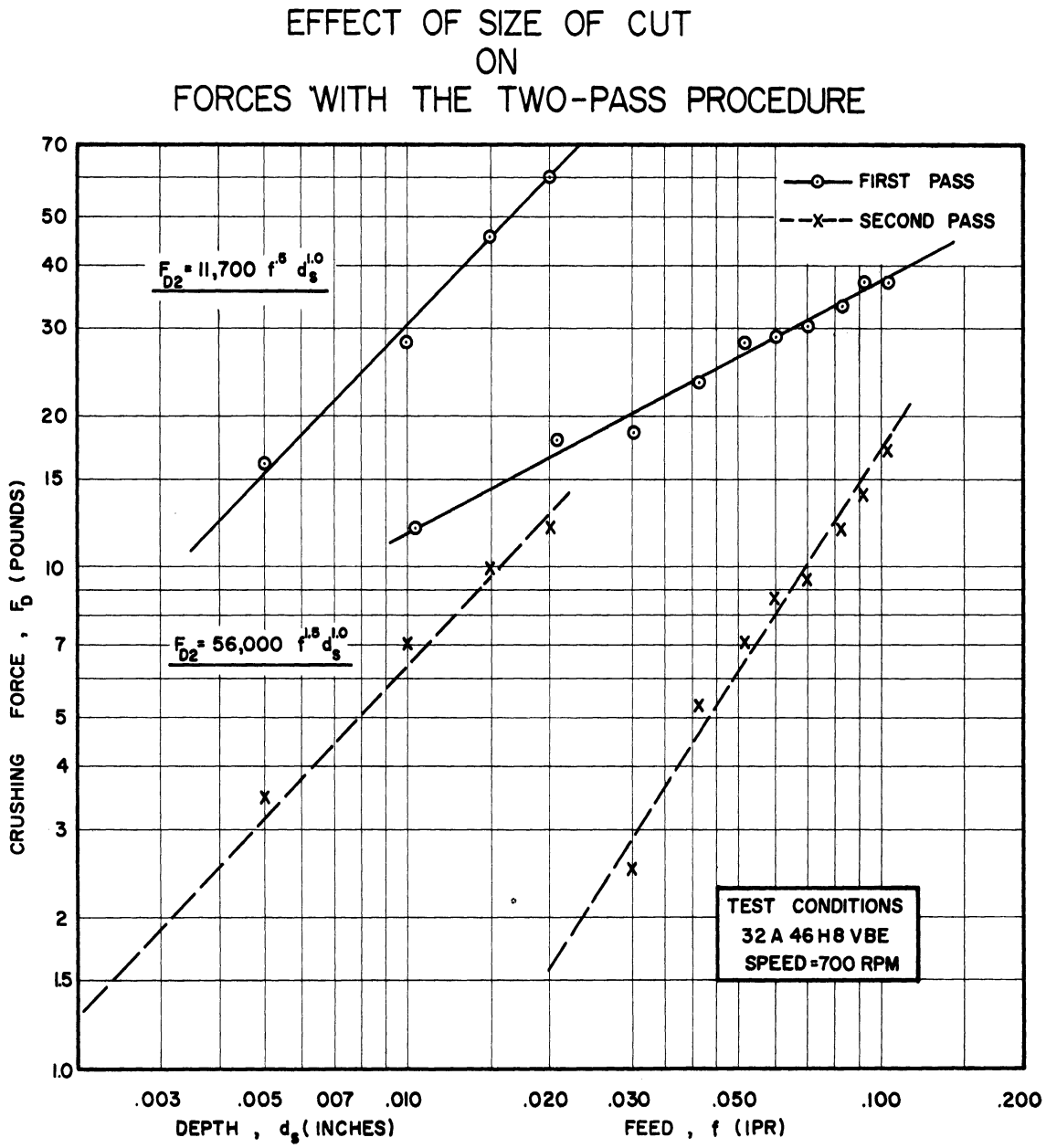

Figure 22. Plot of crushing forces on successive passes in a procedure wherein the cross-slide was adjusted inward on every other pass. Force on second pass reflects residual elastic force present in first pass. The depths shown on the plot are depth settings only. Actual depths of cut are unknown as yet except that the sum for two successive passes equals the depth setting.

is passed across the wheel again at the same feed rate but without changing the depth setting. Any residual elastic deflection from the first pass will cause further crushing on the second pass. This is true also for the third, fourth and any successive additional passes until only finite elastic contact is made. Practically this point will not be reached except at low speeds since the necessity for accelerating the cutter causes the residual depth to be decreased further by actual grinding of the cutter.

The data shown plotted in Figure 22 is for a constant feed of 0.052 ipr when the depth is varied and a constant depth setting of 0.010 inches when the feed rate is varied. It is interesting to note the difference in slope of the two lines representing the first and second passes on variable feed. They intersect at a feed rate of 0.210 ipr which is beyond the 0.100 inch wall thickness of the cutter used. This means that no crushing could occur at feeds equal to or greater than this amount since the contact conditions would be purely elastic and the test would become erratic with successive infeeding.

When the feed rate is held constant at some value below the critical value there will always be some crushing on the first pass however large the infeed may be in which case the force on the second pass will always be less than that for the first pass. Consequently the lines for variable depth at the left in Figure 22 must diverge with increasing depth setting. Theoretically, purely elastic contact will be achieved at some light depth but it is difficult establish the location of such a point at the test conditions used in this preliminary investigation. The lines in Figure 22 were purposely drawn at the slopes represented by the exponents shown because of possible analytical significance. They fit

the data well but it is not yet known whether there is some fundamental reason why they should remain substantially constant or if they should vary in some manner with variations in the grinding wheel and system rigidity. These questions require further exploration and analysis. Such questions become somewhat academic since it already has been established that the two-pass procedure is dependable and repeatable. On the other hand, the answers to these questions will establish the conditions necessary for making a hardness test truly universal.

A range of 12 x 1 x 5 wheels from various sources were tested in the laboratory with the two-pass procedure at only one set of cutting conditions. The resultant first and second pass forces are listed in Table VI. The ratio of the second divided by the first and multiplied by 1000 to avoid decimal points is shown in the fourth column. These values range from a low of 111 to a high of 575 for the vitrified wheels. Both resin bonded wheels gave values over 800 but the lower of these for the C60L11B1268 wheel is questionable because the force on the first pass was so high that the dynamometer chattered violently and probably removed more abrasive than normal because of the resulting impact.

It should be noted that this basis for assigning a hardness number provides a maximum value of 1000. It should be noted also that both hardened steel and soft rubber would yield the same result; a hardness rating of 1000. This is as it should be because neither would break down or crush under load if they were the bonding material and both would act exceedingly hard in actual grinding.

There are some practical problems associated with using the force ratio as a hardness number. These difficulties occur primarily at

TABLE VI

FORCES AND RATIOS FOR TWO-PASS PROCEDURE

Wheel	F_{D1}-Lbs.	F_{D2}-Lbs.	$F_{D2}/F_{D1}(X10^3)$	F_{D1} - %
48A46H8V6	18	2	111	100
-I-	24	3	125	133
-J-	40	14	350	212
-K5-	62	32	515	344
48A46H5V6	41	15	366	228
-60-	50	22	440	278
-80-	90	50	555	500
48A60H8V6	40	10	250	212
(a) 48A60H8V6	41	12	293	228
-12-	54	20	372	300
(a) 48A60H8V6	56	25	446	311
48A60K5V6	87	50	575	483
84A46H8VMM	22	3	136	122
-L8-	40	12	300	212
C60K11B1268	108	92	850	600
-L11-	134	108	810	745
DA60F9V2D	22	2.5	113	122
-G9-	28	5	178	155
-J9-	42	14	343	233
39C60I7V	26	4	154	144
-J7-	34	8	245	189
-K5-	72	40	555	400
32A46H8VBE	28	7	250	155

Test Conditions: Depth Setting: 0.010 inches; Feed: 0.052 ipr; Speed: 700 rpm.

(a) Test on another wheel of the same specification.

low hardness where the force on the second pass approaches zero and small errors in force measurements give rise to large variations in the hardness number. However this can be overcome by proper selection of test conditions.

Other possibilities for forming dimensionless hardness numbers include forming ratios of either force with either the sum or the difference of the two. Still others are possible but the best will be the one which provides an optimum combination of dependability, sensitivity and relevance to the elastic factors involved in grinding wheel behavior.

All of the data in Table VI were plotted on logarithmic coordinates in Figure 23. The second pass forces are plotted vertically against the first pass forces resulting in the equation

$$F_{D2} = C\, F_{D1}^{2.0} \quad .$$

The fact that the test points for all of the wheels lie close to the line would seem to indicate that this correlation is strongly dependent on system rigidity. The coefficient-C and the exponent may both be sensitive to system rigidity and size of cut. These factors are being investigated further in order to resolve these questions.

The Effect of Speed

Figure 24 is a plot of one of several sets of data all of which indicate that surface speed has very little effect on average readings. An attempt was made to filter the high frequency variations in the laboratory instruments in order to get better averages. However, the filtering was inadequate at low speeds, particularly below about 50 rpm. The dashed

PLOT OF FORCES FROM TABLE NO. VI

Errata:

$F_{D2} = CF_{D1}^{2.0}$

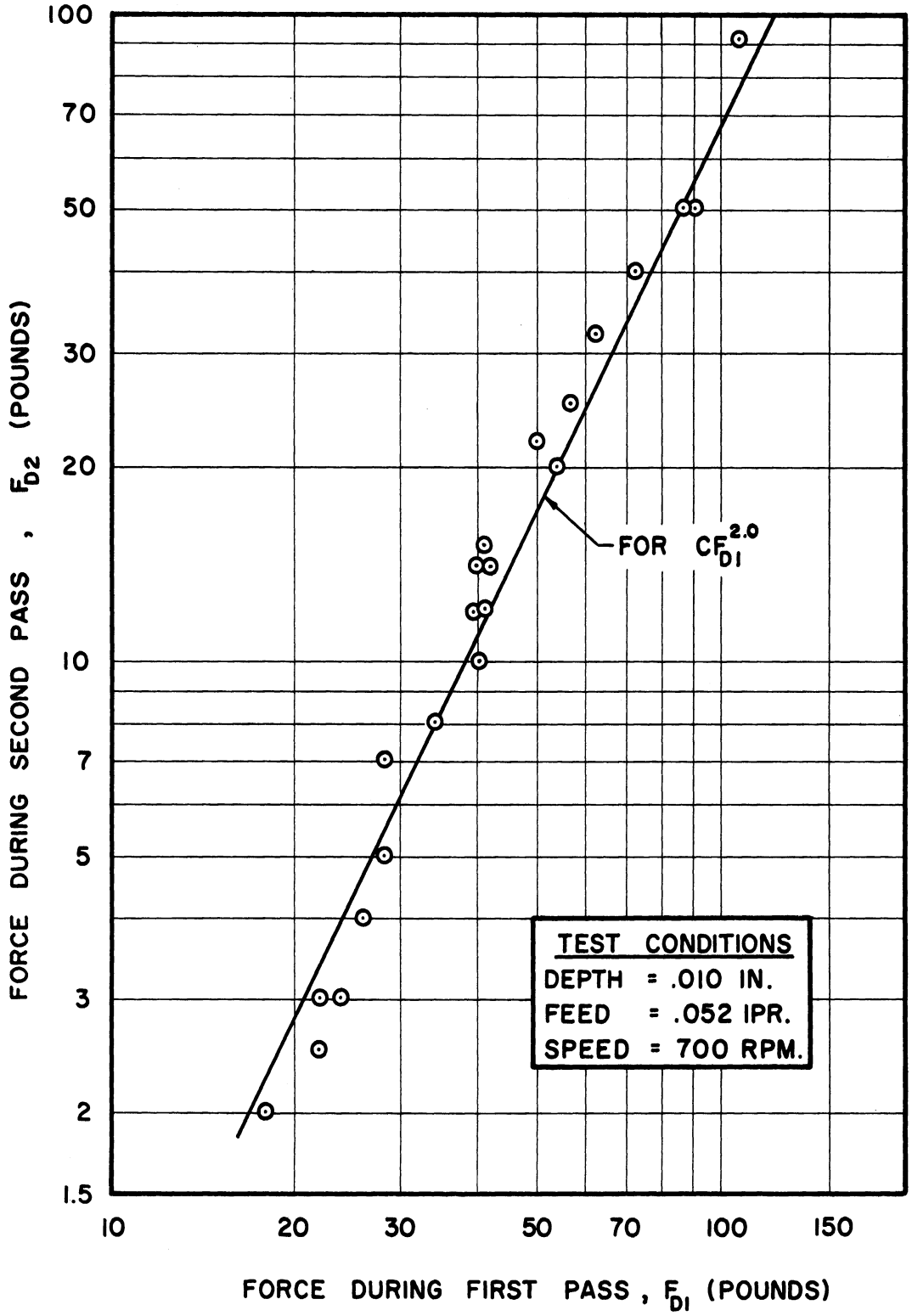

Figure 23. Relationship of force on second pass to that for the first pass in the two-pass procedure. All of the grinding wheels in Table VI are represented by test points. The correlation appears to reflect system rigidity.

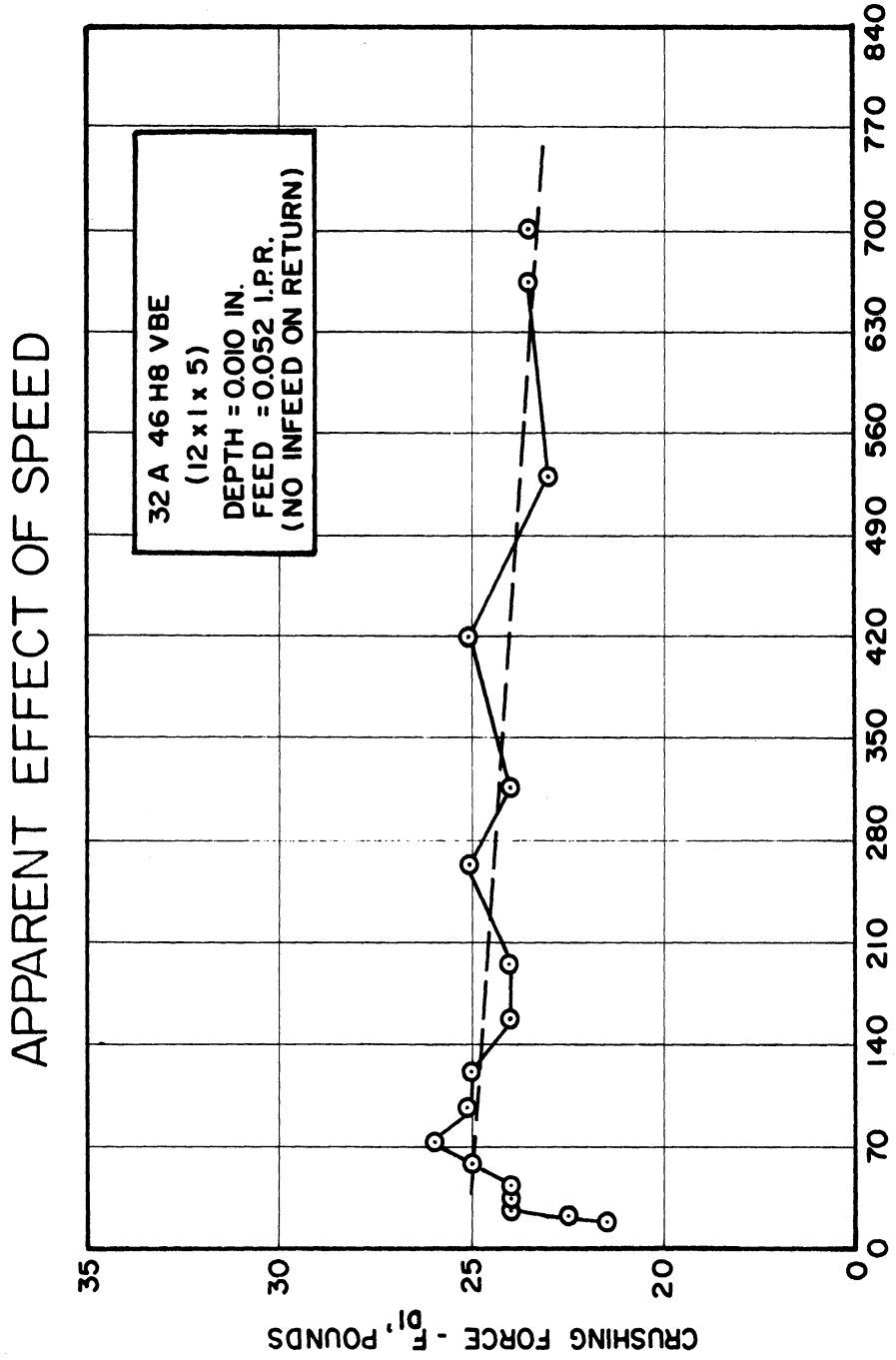

Figure 24. The drop in indicated force with increasing speed in rpm is believed to be due primarily to inability of the recorder pen to keep up with higher frequency force variations. Actual approach speed is less than 10% of surface velocity.

line in Figure 24 indicates that the drop in force level was less than 7% from 70 to 700 rpm and most of this can be attributed to frequency attenuation in the chart recorder. It is also worth noting that the maximum deviation of readings from the dashed line in this same speed range is plus or minus 3 percent which is relatively small considering the low capacity of the improvised filtering.

The relatively minor speed effect is not surprising when one calculates the actual relative speed or speed of approach between the abrasive grains and the crushing wheel. This factor is analysed in Section III of the Appendix and the results show that the maximum approach speed is about 250 fpm at 700 rpm compared to a surface velocity of about 2200 fpm. The corresponding radial approach velocity in actual griding is even less; less than 100 fpm for a heavy cylindrical grinding cut at a wheel speed of 6000 fpm. Therefore it does not appear that there are any impact effects in the crushing process associated with this test.

Summary

The results of the study up to this writing have established several useful facts and show evidence that still more may be evolved. Among those things which are already reasonably well established are that

1) The crush cutting process is orderly and susceptible to precise measurement,
2) The measured forces also are orderly and correlate in a logical manner with the elastic and grain concentration factors which Peklenik has found to be important in actual grinding,

3) The measured forces reflect all of the elastic properties of bonded abrasives as well as those of the entire system,

4) Effective hardness of bonded abrasives involves not only the strength property which determines the force at which a dull abrasive grain will be released but also the soft or elastic factors which tend to aggravate and intensify the deleterious effects of dullness,

5) Grinding wheels can be graded in production competently, quickly and economically and,

6) A universally applicable hardness scale involving dimensionless numbers can be established and corresponding industrial standards can be developed.

Further studies along these same lines can reasonably be expected to produce

a) A basis for predicting chatter conditions in grinding,

b) Information on the effect of machine rigidity on grinding behavior,

c) A basis for predicting differences in performance of the same grinding wheel on different grinding machines,

d) Information on the difference in behavior of the same grinding wheel at different grinding conditions.

APPENDIX

I. Geometry of the Contact Zone

The shape of the contact area between the conical crushing wheel or cutter and the grinding wheel will be defined by the curve of intersection of a plane of the grinding wheel with that of the conical crushing surface as illustrated in Figure A. The equation of any cone with its apex at the origin of cartesian coordinates and with its axis coincident with the Z-axis is

$$X^2 + Y^2 = K^2Z^2 \tag{A-1}$$

where Z must vary in a fixed ratio with X and Y. For this purpose let

$$K^2 = \tan^2\phi = \frac{X^2 + Y^2}{Z^2} \tag{A-1a}$$

where ϕ is one half the included angle of the cone.

In order to simplify the equation of the intersection of the cone with a plane of the grinding wheel, it is desirable to rotate the coordinate axes counterclockwise about the Y-axis until the Z-axis becomes an element of the cone. For this purpose, the following substitutions must be made in Equation (A-1a)

$$X = Z' \sin\phi + X' \cos\phi$$

$$Z = Z' \cos\phi - X' \sin\phi$$

$$Y = Y'$$

Substituting and then dropping the prime symbol gives rise to

$$Z \sin^2\phi + 2ZX \sin\phi \cos\phi + X^2 \cos^2\phi + Y^2 =$$

$$\tan^2\phi \, (Z^2 \cos^2\phi - 2ZX \sin\phi \cos\phi + X^2 \sin^2\phi)$$

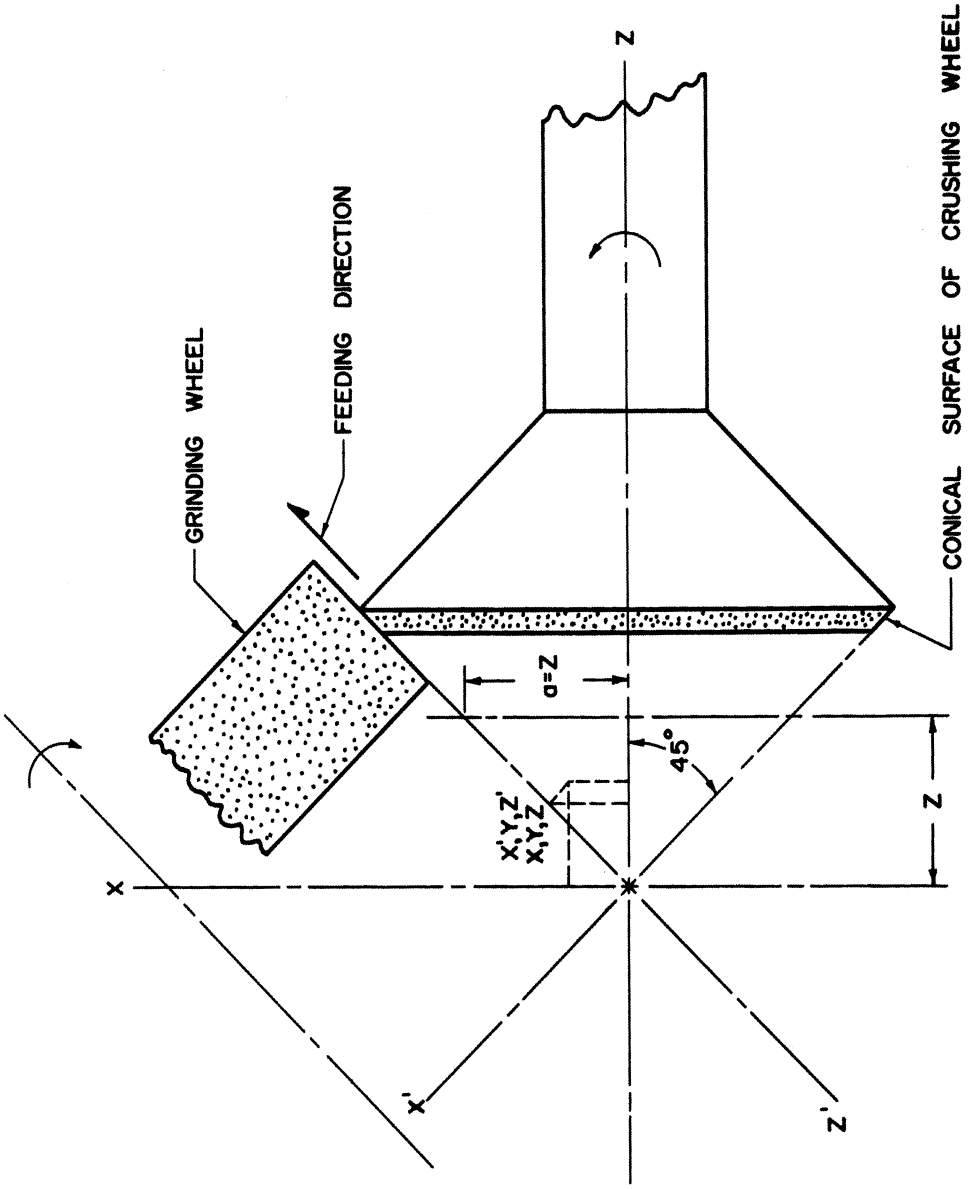

Figure A. Illustrates the essential geometry in the crushing zone. The conical surface of the crushing wheel produces a parabolic surface in the plane of the grinding wheel.

which simplifies for the general case to

$$X^2 \left(\frac{\cos^4\phi - \sin^4\phi}{\cos^2\phi}\right) + Y^2 = -2ZX \left(\frac{\sin^3\phi + \sin\phi \cos^2\phi}{\cos\phi}\right) \quad (A\text{-}2)$$

When, as in this case, the included angle of the cone is 90 degrees, then ϕ = 45 degree, sin ϕ = cos ϕ and Equation (A-2) reduces to

$$Y^2 = -2ZX \quad (A\text{-}3)$$

which is a parabola with a radius of curvature equal to Z at its apex. Consequently the crushing wheel is essentially a cylinder or circular disc of the same radius-Z. The original diameter of the wheels is three inches so that if they are used until worn down to 2.750 inches the average radius of curvature in the contact zone will average about two inches so that

$$Y^2 = 4X \quad (A\text{-}4)$$

where X is treated as a positive number proportional to the radial depth of contact with the grinding wheel.

II. Area of the Contact Zone

The area of the contact zone wherein crushing takes place is a function of the feed rate (f-ipr), the radial depth (d-inches) and the relative geometry of grinding and crushing wheels as illustrated in Figure-B. The actual arc of contact is so small (less than 7 degrees) that the difference between arc length and the height of the intercept Y_1 in Figure-B is negligible and the area under crushing influence (A_c) can be expressed as

$$A_c = fY_1 \text{ (in.}^2\text{)} . \quad (B\text{-}1)$$

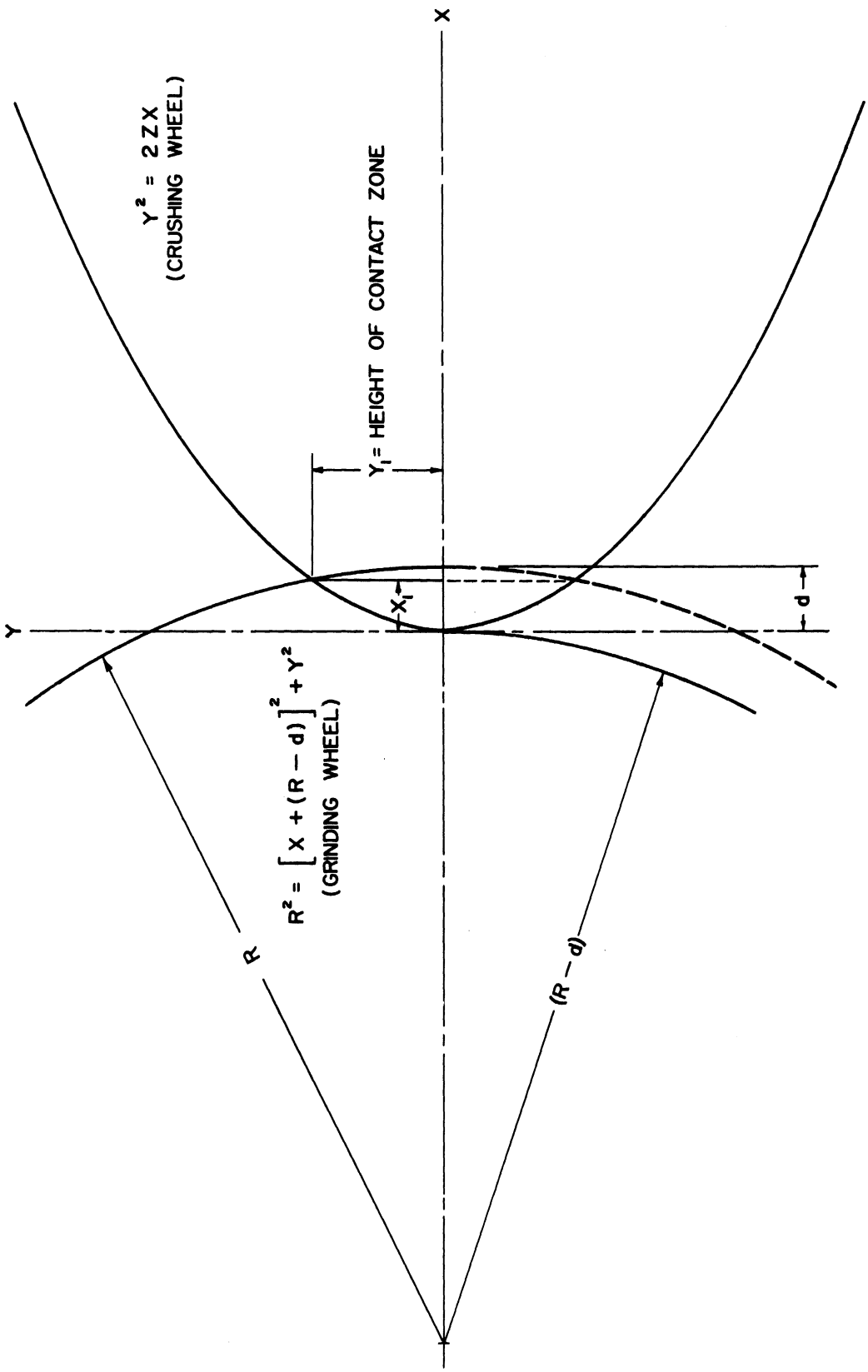

Figure B. Shows the geometric relationship between the radial crushing depth-d and the height-Y_1 of the contact zone. The area being crushed is f Y_1 where -f is the feed rate in ipr. The feed -f is in a direction perpendicular to the plane of the sketch.

It is necessary to develop the relationship between the intercept-Y_1 and the depth of cut-d. This can be done substituting the equation of the parabola (A-3) into the equation for the grinding wheel

$$R^2 = [X + (R-d)]^2 + Y^2 \qquad (B-2)$$

where the origin-0 is at the nose of the parabola and the center of the grinding wheel is placed on the X-axis at a distance (R-d) inches to the left of the origin.

Substituting (A-3) into (B-2) gives

$$X_1^2 + 2(Z + R - d)X + d^2 - 2Rd = 0 \; . \qquad (B-3)$$

Solving (B-3) for X_1 gives

$$X_1 = \pm\sqrt{(R+Z)^2 - 2Zd} - (R+Z-d) \; . \qquad (B-4)$$

Equation (B-4) was used calculate the values shown in Table-A below for the range of depth of cut used in this investigation. The radius-Z was held constant at two inches.

TABLE-A

VALUES OF X_1 AND Y_1 AT TEST CONDITIONS

	R = 6 in.		R = Infinity	
Depth-d(ln)	X_1-ln	Y_1-ln	X_1-ln	Y_1-ln
0.0025	.00187	.0870	.0025	.1000
0.005	.00375	.1225	.005	.1414
0.010	.00750	.1732	.010	.2000
0.015	.01125	.2121	.015	.2450
0.020	.01500	.2449	.020	.2828

The values in the above table for R equal to infinity are applicable to flat surfaces of cup wheels, honing stones etc. It will be noted that for the limited range of depths that X_1 remained constant at three quarters of the corresponding depth. Consequently, 0.75d can be substituted for X in Equation (A-4) so that the equation for the area under crushing influence becomes

$$A_c = \sqrt{3}\ f\ d^{.5}\ (in.^2) \qquad (B\text{-}5)$$

where:

f = feed rate (ipr)

d = depth (in)

III. Velocity of Approach

The relative velocity with which the abrasive grains and the crushing wheel approach each other can be determined easily in view of the fact that both have the same surface velocity-V. It will be the sum of the X-axis components in reference to Figure B.

a) Crushing Wheel Component - V_c

$$V_c = \frac{Y_1}{Z}\ V = \frac{\sqrt{2ZX}}{Z}\ V \qquad (C\text{-}1)$$

for the general case and

$$V_c = \frac{\sqrt{3}}{2}\ d^{.5}\ V \qquad (C\text{-}2)$$

for the conditions used in this investigation.

b) Grinding Wheel Component - V_g

$$V_g = \frac{Y_1}{R} V = \frac{\sqrt{2ZX}}{R} V \qquad (C\text{-}3)$$

for the general case and

$$V_g = \frac{\sqrt{3}}{6} d^{.5} V \qquad (C\text{-}4)$$

for the conditions used in this investigation

c) The Total Relative Velocity - V_r

$$V_r = V_c + V_g$$

$$V_r = \frac{\sqrt{3}}{2} d^{.5} V + \frac{\sqrt{3}}{6} d^{.5} V = \frac{2}{3}\sqrt{3} d^{.5} V$$

$$V_r = 1.152 d^{.5} V \qquad (C\text{-}5)$$

Typical approach velocities at test conditions are summarized in the following table for 12 inch diameter grinding wheels.

TABLE-B

APPROACH VELOCITIES DURING CRUSHING

Depth-d(in)	At 700 rpm	At 319 rpm
.0025	127 fpm	58 fpm
.005	180	81
.010	254	115
.020	360	162

During actual cylindrical grinding of a 4 inch diameter with a 12 inch diameter grinding wheel at 6000 fpm surface speed, the corresponding approach velocities would be 87 fpm for a heavy depth of 0.0025 inch and only 39 fpm for a depth of 0.0005 inch.

IV. Elastic Contact Conditions

At most of the test conditions there is a substantial elastic component in the total force. This component cannot be reduced below a value corresponding to the average minimum fracture stress and the latter is a function of the elastic properties of the bonded abrasive as well as the magnitude of the applied load.

These relationships can be approximated by assuming that the abrasive wheel is a continuous and homogeneous material in which case the equations for contact stresses between rolling cylinders are applicable. Timoshenko(a) gives the following equations for cylinders with parallel axes:

$$b^2 = \frac{4P'(k_1+k_2)R_1R_2}{R_1+R_2} \qquad \text{(D-1)}$$

$$q_o^2 = \frac{P'(R_1+R_2)}{\pi^2(k_1+k_2)R_1R_2} \qquad \text{(D-2)}$$

where:

R_1 and R_2 = radii of the cylinders - in.

b = half the width of the area of contact - in.

q_o = maximum pressure in contact area - psi.

P' = normal force - lbs/in of contact length

(a) "Theory of Elasticity," by S. Timoshenko, McGraw-Hill Book Company, 1934, p. 349.

$$k = \frac{1-\nu^2}{\pi E}$$

ν = Poisson's Ratio

E = modulus of elasticity .

TABLE-C

ELASTIC PROPERTIES OF WHEELS

Type of Wheel	E psi	ν	k
Vitrified Abrasive	14×10^6	0.18	22×10^{-9}
Resinoid Abrasive	3.5×10^6	0.235	86×10^{-9}
Steel Cutter	30×10^6	0.3	9.65×10^{-9}

Comparative values of pressure and width of contact for resinoid and vitrified wheels in contact with steel cutters were calculated by inserting quantities from Table C into Equations (D-1) and (D-2). The grinding wheel radius was set equal to six inches and cutter wheel radius was taken as two inches. Conditions were calculated for elastic components of 10 pounds and 100 pounds. The results are summarized in Table D.

TABLE D

A COMPARISON OF CONTACT PRESSURES AND AREAS
FOR
(Vitrified and Resinoid Grinding Wheels)

	10 pound load		100 pound load	
	2b-in.	q_o-psi	2b-in.	q_o-psi
Vitrified Wheel	.0087	14,600	.0276	46,150
Resinoid Wheel	.0151	8,500	.0478	26,700

Table D shows that for the same load the maximum pressures for vitrified wheels are nearly twice as high as for resinoid wheels and the areas are only slightly more than half as wide. From another viewpoint resinoid wheels will require a higher elastic force component and therefore a higher total force for the same crushing strength. A comparison of the loads-P' for the same maximum pressure-q_o shows that resinoid wheels would require approximately three times as high a load.

It should be noted that the widths-2b in Table D range from 0.0087 to 0.0478 which would permit only a few grains to be in contact with the wheel. This means that the actual projected areas must be somewhat larger and that the maximum pressures may be much higher than would be determined from equation. However, the relative values of actual load, pressure and area as between resinoid and vitrified wheels must be substantially the same as indicated in the above analysis.

BIBLIOGRAPHY

1. "Ermittlung von geometrischen und physikalischen Kenngrossen fur die Grundlagenforschung des Schleifens." von Dr.-Ing. Janez Peklenik, 1957. A dissertation from the Technische Hochschule in Aachen, Germany.

2. "Grundlagen der Theorie des Metallschleifens." Verlag "Technik," Berlin, Germany, 1952.

3. "Grinding Workmaterials and their Manufacture." V.J. Ljubomudrov and others. Masgis, 1953.